Development of Impulsive Noise Detection Schemes for Selective Filtering in Images

Subrajeet Mohapatra

Department of Computer Science and Engineering
National Institute of Technology Rourkela
Rourkela–769 008, Orissa, India

September 2008

Development of Impulsive Noise Detection Schemes for Selective Filtering in Images

Thesis submitted in partial fulfillment
of the requirements for the degree of

Master of Technology
(Research)

in

Computer Science and Engineering

by

Subrajeet Mohapatra
(Roll: 60606004)

Department of Computer Science and Engineering
National Institute of Technology Rourkela
Rourkela–769 008, Orissa, India

September 2008

Department of Computer Science and Engineering
National Institute of Technology Rourkela
Rourkela–769 008, Orissa, India.

Certificate

This is to certify that the work in the thesis entitled *Development of Impulsive Noise Detection Schemes for Selective Filtering in Images* by *Subrajeet Mohapatra* is a record of an original research work carried out by him under our supervision and guidance in partial fulfillment of the requirements for the award of the degree of Master of Technology (Research) in Computer Science and Engineering during the session 2006–2008 in the department of Computer Science and Engineering, National Institute of Technology Rourkela. Neither this thesis nor any part of it has been submitted for any degree or academic award elsewhere.

Rameswar Baliarsingh
Assistant Professor
CSE department of NIT Rourkela

Banshidhar Majhi
Professor
CSE department of NIT Rourkela

Place: NIT Rourkela
Date: 08 January 2009

Acknowledgment

It will be simple to name all those people who helped me to get this thesis done, however it will be tough to thank them enough. I will nevertheless try...

I would like to gratefully acknowledge the enthusiastic supervision and guidance of Prof. Banshidhar Majhi for the ideas that led to this work, for his timely comments, guidance, support and patience throughout the course of this work. He is my source of inspiration.

I am grateful to my co-supervisor Prof. R. Baliarsingh for his valuable suggestions, and encouragements during this research period.

I am very much indebted to Prof. S. K. Jena for his continuous encouragement and support. My sincere thanks goes to Prof. S. K. Rath for motivating me to work harder.

Prof. A. K. Turuk and Prof. B. D. Sahoo were like two ceaseless source of power for me. Their help can never be penned with words.

My sincere thanks goes to Prof. P.K. Nanda for his continuous encouragement. I also thank Prof. J.K. Satpathy for serving on my Master Scrutiny Committee.

My overwhelming thanks goes to Prof. S. K. Patra, Prof. G. K. Panda, Prof. D. P. Mahapatra, Prof. P. M. Khilar and Prof. S. Chinara, for being my knowledge resource. Special thanks goes to Prof. P. K. Sa and Mr. R.Dash for appraising my work critically.

I thank to all my friends for being there whenever I needed them. Thank you very much Mrinal, Dilip, Swasti, Hunny, Baikuntha, Prem, Bandana, Jayprakash, Dheeraj. I have enjoyed every moment I spent with you.

I must acknowledge the academic resource that I have got from NIT Rourkela.

Finally, I am forever indebted to my parents and my sister for their understanding and encouragement when it was most required.

Subrajeet Mohapatra

Abstract

Image Noise Suppression is a highly demanded approach in digital imaging systems design. Impulsive noise is one such noise, which is frequently encountered problem in acquistion, transmission and processing of images. In the area of image restoration, many state-of-the art filters consist of two main processes, classification (detection) and reconstruction (filtering). Classification is used to separate uncorrupted pixels from corrupted pixels. Reconstruction involves replacing the corrupted pixels by certain approximation technique. In this thesis such schemes of impulsive noise detection and filtering thereof are proposed.

Impulsive noise can be *Salt & Pepper Noise* (SPN) or *Random Valued Impulsive Noise* (RVIN). Only RVIN model is considered in this thesis because of its realistic presence. In the RVIN model a corrupted pixel can take any value in the valid range.

Adaptive threshold selection is emphasized for all the four proposed noise detection schemes. Incorporation of adaptive threshold into the noise detection process led to more reliable and more efficient detection of noise. Based on the noisy image characteristics and their statistics, threshold values are selected.

To validate the efficacy of proposed noise filtering schemes, an application to image sharpening has been investigated under the noise conditions. It has been observed, if the noisy image passes through the sharpening scheme, the noise gets amplified and as a result the restored results are distorted. However, the prefiltering operations using the proposed schemes enhances the result to a greater extent.

Extensive simulations and comparisons are done with competent schemes. It is observed, in general, that the proposed schemes are better in suppressing impulsive noise at different noise ratios than their counterparts.

List of Acronyms

Acronym	Description
AHE	Adaptive Histogram Equalisation
CV	Coefficient of Variance
CV	Coefficient of Variance Adaptive Thresholding
DCT	Discrete Cosine Transform
FLANN	Functional Link Artificial Neural Network
FP	False Positive
FN	False Negative
ISAT	Image Statistics based Adaptive Thresholding
MLP	Multilayer Perceptron
MLPAT	Multilayer Perceptron based Adaptive Thresholding
MSE	Mean Square Error
PSNR	Peak Signal to Noise Ratio
PSP	Percentage of Spoiled Pixels
RBFN	Radial Basis Functional Network
RBFNAT	Radial Basis Functional Network based Adaptive Thresholding
SPN	Salt and Pepper Noise

List of Symbols

Symbol	Description
μ	Statistical Mean of the Image
γ	Standard Deviation
γ^2	Variance
λ	Amplification factor
η	Noise
θ_{opt}	Optimum Noise Threshold value
c	Constant Factor
L	Maximum Gray Level of an Image
p	Noise Probability
r	Value of Image Pixel before Processing
s	Value of Image Pixel after Processing

List of Figures

1.1 Image Processing Tree 4

1.2 (a) Model of the image degradation/restoration process, (b) Model of the Noise Removal Process. 13

1.3 Nonlinear Filter Family 15

1.4 Representation of (a) *Salt & Pepper Noise* with $R_{i,j} \in \{n_{min}, n_{max}\}$, (b) *Random Valued Impulsive Noise* with $R_{i,j} \in [n_{min}, n_{max}]$ 18

1.5 PSNR (dB) variations of *Lena* image corrupted with RVIN by Group-A schemes 37

1.6 PSNR (dB) variations of *Lena* image corrupted with RVIN by Group-B schemes 37

1.7 PSNR (dB) variations of *Lena* image corrupted with RVIN by Group-C schemes 38

1.8 PSP variations of *Lena* image corrupted with RVIN by Group-A schemes 38

1.9 PSP variations of *Lena* image corrupted with RVIN by Group-B schemes 39

1.10 PSP variations of *Lena* image corrupted with RVIN by Group-C schemes 39

1.11 PSNR (dB) variations of *Lena* image corrupted with SPN 40

1.12 PSP variations of *Lena* image corrupted with SPN 40

1.13 Subjective Evaluation of *Lena* image subjected to Cascaded Noise Reduction and Sharpness Enhancement schemes 41

2.1 Gray level profile, first-order and second-order derivative of an image 44

2.2 Window Selection for an $M \times N$ Image 47

2.3 Variation of MSE for different threshold values for 1% RVIN noise for *Lena* image. 48
2.4 Variation of Optimum threshold for different noise % for *Lena* image. 48
2.5 Variation of Minimum MSE at different Threshold values 49
2.6 Variation of Optimum threshold with CV at different noise density for *Lena* image. 50
2.7 Multi-Layer Perceptron Structure of Threshold (θ_1) Estimator. . . . 52
2.8 Convergence Characteristics of Multilayer Perceptron Network . . . 53
2.9 Functional Link Artificial Neural Network (FLANN) Structure for Threshold Estimation 54
2.10 Convergence Characteristics of FLANN structure 55
2.11 Radial Basis Functional Network (RBFN) Structure for Threshold Estimation 56
2.12 Convergence Characteristics of Radial Basis Functional Network . . 57
2.13 PSNR (dB) variations of Restored *Lena* image corrupted with RVIN of varying strengths by different adaptive threshold schemes 58
2.14 PSP variations of Restored *Lena* image corrupted with RVIN of varying strengths by different adaptive threshold schemes 61
2.15 Impulsive Noise filtering of *Lena* image corrupted with 15% of RVIN by different adaptive threshold schemes 62
2.16 Impulsive Noise filtering of *Peppers* image corrupted with 20% of RVIN by different adaptive threshold schemes 63

3.1 Variation of Minimum MSE at different Threshold values 66
3.2 Functional Link Artificial Neural Network (FLANN) Structure for Threshold Estimation using CV 69
3.3 Convergence Characteristics of the CV based FLANN 69
3.4 PSNR (dB) plot of Restored *Lena* image corrupted with RVIN of varying strengths 72
3.5 PSP plot of Restored *Lena* image corrupted with RVIN of varying strengths 73

3.6 Subjective comparison of impulsive noise removal of *Lena* image corrupted with 15% of RVIN by different filters 73
3.7 Subjective comparison of impulsive noise removal of *Peppers* image corrupted with 20% of RVIN by different filters 74

4.1 Variation of PSNR (dB) at different RVIN percentage on *Lena* image. 78
4.2 Computational time of proposed schemes for *Lena* (512×512) with 15% RVIN. 79

5.1 Linear Unsharp Masking scheme 82
5.2 Improved Unsharp Masking scheme 83
5.3 Comparison among different enhancement approaches for *Lena image* 84
5.4 Comparison among different enhancement approaches for *Pepper image* 85

List of Tables

1.1 Comparative Results in PSNR (dB) of different filters for *Lena* image corrupted with RVIN of varying strengths 35

1.2 Comparative Results in PSP of different filters for *Lena* image corrupted with RVIN of varying strengths 36

2.1 PSNR (dB) of different adaptive schemes at 15% and 20% of noise on different images 59

2.2 PSP of different adaptive schemes at 15% and 20% of noise on different images 60

2.3 Computational time for different Schemes for removing impulsive noise from *Lena* image corrupted with 15% of RVIN 60

3.1 PSNR (dB) of different schemes at 15% and 20% of noise on different images 71

3.2 PSP of different schemes at 15% and 20% of noise on different images 71

3.3 Computational time consumed by different Schemes for removing impulsive noise from *Lena* image corrupted with 15% of RVIN . . 71

4.1 Noise classification as per noise ratio 75

4.2 Noise removal scheme chosen for comparison 76

4.3 False Positive Percentage(FP%) and False Negative Percentage (FN%) of proposed schemes for Lena (512×512) with 15% RVIN. 77

4.4 Basis of comparison among the filtering schemes 77

4.5 Comparison of schemes under low and medium noise conditions . . 78

4.6 Comparison of different schemes under high noise conditions 78

4.7 Computational overhead per pixel associated in filtering schemes . 79

Chapter 1

Introduction

Within seconds of entering the world, those who are blessed with the gift of sight start acquiring images. Human beings are primarily visual creatures who depends solely on sense of vision. So vision allows humans to perceive and understand the world surrounding them in a better manner. Hence, processing visual information by computer has been drawing a very significant attention of the researchers over the last few decades. The process of receiving and analyzing visual information by the human species is referred to as sight, perception or understanding. Similarly, the process of receiving and analyzing visual information by digital computer is called *digital image processing* [1]. Before advancing more we should answer one question *"Why do we process images ? "*

Image Processing has been developed in response to solve three major problems concerned with pictures [2]:

- Picture digitization and coding to facilitate transmission, printing and storage of pictures.
- Picture enhancement and restoration in order for example, to interpret more easily pictures of the surface of other planets taken by various probes.
- Picture segmentation and description as an early stage in machine vision.

An image may be described as a two-dimensional function I.

$$I = f(x, y) \tag{1.1}$$

where x and y are spatial coordinates. Amplitude of f at any pair of coordinates (x, y) is called intensity I or gray value of the image. When spatial coordinates

and amplitude values are all finite, discrete quantities, the image is called digital image [3]. The digital image I is represented by a single 2- dimensional integer array for a gray scale image and a series of three 2- dimensional arrays for each colour bands.

Digital image processing may be classified into various subbranches based on methods whose [3]:

- input and output are images and
- inputs may be images where as outputs are attributes extracted from those images.

Following is the list of different image processing functions based on the above two classes.

- Image Acquisition
- Image Enhancement
- Image Restoration
- Color Image Processing
- Multi-resolution Processing
- Compression
- Morphological Processing
- Segmentation
- Representation and Description
- Object Recognition

For the first seven functions the inputs and outputs are images where as for the rest three the outputs are attributes from the input images. With the exception of image acquisition and display most image processing functions are implemented in software. Image processing is characterized by specific solutions, hence

the technique that works well in one area can be inadequate in another. The actual solution of a specific problem still requires a significant research and development [4]. Among the broad spectrum of applications remote sensing, medical imaging, image morphing and warping are important. Figure 1.1 [2] depicts a pictorial representation of various image processing applications along with different image processing functions.

Out of the ten sub-branches of digital image processing, cited above, this thesis deals with image restoration and one of its application to enhancement. To be precise, the thesis devotes on a part of the image restoration i.e. noise removal from images, stated in the Problem Definition. Further, this thesis also discusses how image noise removal can be utilized for high quality image enhancement.

This chapter is organized as follows. Section 1.1 is devoted to convey the basic concepts of Image Enhancement and its various types, problems associated with enhancement techniques are presented in Section 1.4. Image Restoration is discussed in Section 1.2 followed by a broad classification of filters in Section 1.3. The problem definition associated with noise removal from images is described in Section 1.4. Different performance measures for comparison are described in Section 1.5. Review of different existing schemes and their performance analysis is done in Section 1.6. Motivation behind carrying out the work is stated in Section 1.7. Organization of the thesis is outlined in Section 1.8. Finally, Section 1.9 provides the chapter summary.

1.1 Image Enhancement

Images are captured at low contrast in a number of different scenarios. The main reason for this problem is poor lighting conditions (e.g., pictures taken at night or against the sun rays). As a result, the image is too dark or too bright, and is inappropriate for visual inspection or simple observation. Image enhancement algorithms are used in a variety of image processing applications, primarily to improve or enhance the visual quality of an image by accentuating certain features [5]. Image processing modifies pictures to improve them (enhancement, restoration) to

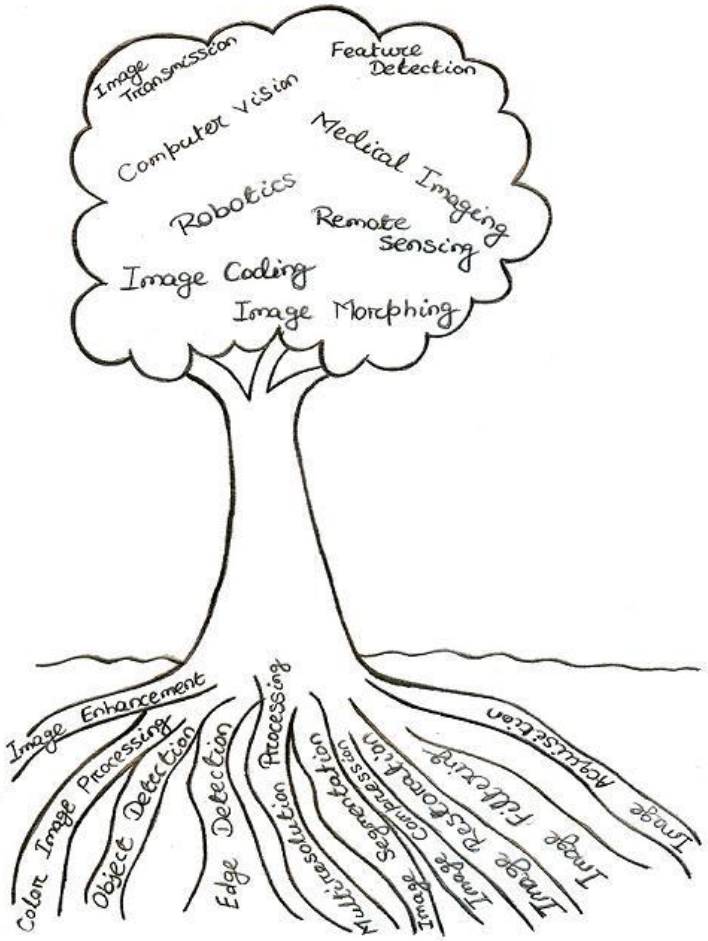

Figure 1.1: Image Processing Tree

prepare suitable images for various applications from raw unprocessed images. Images can be processed by optical, photographic, and electronic means, but image processing using digital computers is the most common method because digital methods are fast, flexible, and precise. Image enhancement improves the quality (clarity) of images for human viewing. Increasing contrast, and revealing details are examples of enhancement operations where as removing blurring and noise comes under the category Image restoration.

Planetary scientists were the first users of enhancement techniques to enhance images of Mars,Venus and other planets. Radiologists, Doctors use this technology frequently to manipulate CAT scans, MRI and X-ray images. Areas like forensic science use image sharpening(enhancement) techniques for criminal detection. Enhancement algorithms are used extensively to enhance biometric (finger print,

iris) images in airport, banking security systems. Palm print manuscripts contain religious texts and treaties on a host of subjects such as astronomy, astrology, architecture, law, medicine and music. Most of these palm-leaves are nearing the end of their natural lifetime or are facing destruction from elements such as dampness, fungus, ants and cockroaches. enhancement algorithms are inevitable members of the preservation projects to protect these valuable historical documents. Enhancement techniques are used to enhance the degraded documents so as to enable retrieval of the written text from these documents. Printing technology also uses extensively the enhancement schemes to produce high quality photographic prints. Acquisition of information of an object or phenomenon, by the use of sensing devices that is not in physical or intimate contact with the object i.e forest, vegetation, land utilization, sea changes etc. Various image processing techniques are involved in analyzing the acquired data. Image enhancement is one of the important image processing functions primarily done to improve the appearance of the imagery to assist in visual interpretation and analysis. Image restoration and enhancement are used usually in synchronization rather than as an individual.

This class of image processing algorithms include image sharpening, contrast and edge enhancement. Among the enhancement algorithms contrast enhancement is most important because it plays a fundamental role in the overall appearance of an image to human being. A human being's perception is sensitive to contrast rather than the absolute values themselves. So it is justified to increase the contrast of an image for better perception. Section 1.1.1 provides a detail classification for conventional enhancement schemes under the heading contrast enhancement. This thesis devotes on image sharpening under impulse noise conditions. We concentrate on those noise removal algorithms which preserve edge details as well remove noise using selective filtering technique. This helps the enhancement schemes to be cascaded along with noise removal algorithm to produce better quality images with more edge details.

1.1.1 Contrast Enhancement

Image enhancement usually employs various contrast enhancement schemes to increase the amount of visual perception. Different enhancement schemes emphasize different properties or components of images [1, 3]. Contrast enhancement techniques can be broadly classified into two categories. For the first category, the gray value of each pixel is modified based on the statistical information of the image. Power law transform [6], log transform [6], histogram equalization belong to this category. In the second category the contrast is enhanced by first separating the high and/or low frequency components of the image, manipulating them separately and then recombining them together with the different weights. Unsharp Masking (UM) which emphasizes high frequency components of an image belongs to this category. The pitfalls associated with unsharp masking is presented in problem definition (1.4). One possible solution for this problem is narrated in chapter 5. Some of the contrast enhancement methodologies are described below.

- *Image Negative*

  The negative of an image with gray levels in the range [0, L-1] is obtained by using the negative transformation, which is given by the equation 1.2.

  $$s = L - 1 - r \tag{1.2}$$

  where r & s denote the values of pixels before and after the processing and L is the maximum Gray level intensity of the input image. Reversing the intensity level of an image in this manner produces the equivalent of a photographic negative. This type of processing is particularly suited for enhancing white or gray detail embedded in dark regions of an image.

- *Logarthimic law*

  This is one of the simplest enhancement technique. It uses a log transform to convert the input gray level to an output gray level to expand the values

of dark pixels in an image while compressing higher level values. The general form of the log transformation can be represented using the relation:

$$s = c.\log(1 + r) \tag{1.3}$$

where c is a constant and it is assumed that $r \leq 0$. Where r and s are input and output gray levels respectively.

- *Power Law*

  Devices used for image capture, printing, and display respond according to a power law given as:

  $$s = c.r^{\gamma} \tag{1.4}$$

  By convention, the exponent in the power law equation is referred to as gamma. The process used to correct this power law response is called gamma correction. Images not corrected properly can look bleached out or dark. So proper gamma adjustment must be done to produce the gray levels accurately and produce appropriate brightness.

- *Histogram Equalization*

  The luminance histogram of a typical natural scene that has been linearly quantized is usually highly skewed toward the darker levels; a majority of the pixels possess a luminance less than the average. In such images, detail in the darker regions is often not perceptible. One means of enhancing these types of images is a technique called histogram modification, in which the original image is rescaled so that the histogram of the enhanced image follows some desired form [6]. This method also assumes the information carried by an image is related to the probability of occurrence of each gray level. To maximize the information, the transformation should redistribute the probabilities of occurrence of the gray level to make it uniform. In this way, the contrast at each gray level is proportional to the height of the image histogram [7]. Various modifications of histogram equalization are

also available which increases its potential of contrast enhancement. Adaptive histogram equalization (AHE) [8], Contrast limited adaptive histogram equalization (CLAHE) [9] belong to that category which apply histogram equalization locally on the image and provides better contrast.

- *Unsharp Masking*

  Unsharp masking (UM) is an image manipulation technique which was first used in Germany in the 1930s as a way of increasing the acutance, or apparent sharpness, of photographic images. In Unsharp masking scheme, a high pass filtered scaled version of an image is added to the image itself. It is desired when a particular application requires the high frequency components of an image. One of its principal application is dark room photography [3]. The process can be represented with the help of the following equation.

$$I'_{x,y} = I_{x,y} + \lambda I''_{x,y} \tag{1.5}$$

  where $I_{x,y}$, $I'_{x,y}$ are original and enhanced images respectively. $I''_{x,y}$ is the high pass component of the original image which is scaled with an amplification factor λ as per requirement to obtain the enhanced image $I'_{x,y}$.

1.2 Image Restoration

The field of digital image restoration had its first encounter with the starting of space program by the scientists involved of United States of America and the former Soviet Union in the 1950s and early 1960s. The first images of the Earth, Moon (mainly of the opposite side), and planet Mars were, at that time, of unimaginable resolution which were obtained under big technical difficulties. These programs were responsible for producing many incredible images of our solar system, which were at that time unimaginable. However, the images obtained from the various planetary missions of the time were subject to many photographic degradations. The need to retrieve as much information as possible from such degraded images was the aim of the early efforts to adapt the one-dimensional signal processing algorithms to images, creating a new field that is today known as digital image

restoration. The 22 pictures produced during the Mariner IV flight to Mars in 1964 were later estimated to cost almost $10 million just in terms of the number of bits transmitted alone [10].

In astronomical imaging the ultimate goal is to recover the original celestial image from the degraded one. The degradations were as a result of relative motion between camera and the original scene, defocusing of the lens system because of vibration in machinery and spinning and tumbling of the spacecraft or because of substandard imaging environment. In addition to blurring the space images are also corrupted with additive random noise. Rapidly changing refractive index of the atmosphere was also one of the reasons for the degradation. Pictures from the manned space mission were also blurred due to the inability of the astronaut to steady himself in a gravitation less environment while taking photographs. Extraterrestrial observations were degraded by motion blur as a result of slow camera shutter speed, relative to rapid spacecraft motions. The degradation of images was no small problem. Any loss of information due to image degradation is devastating as it reduces the scientific value of these images. There is no surprise that astronomical imaging is still one of the primary applications of digital image restoration today.

The rapid growth of medical imaging equipment which capture, record, and redisplay in a non-invasive manner the internal structure of living matter or patients, has composed a great challenge and opportunity to image processing tasks. Providing better diagnosis facility would have been a tedious job without image restoration. X-rays, mammograms, and digital angiographic images [11] without filtering would have been of no use since the acquiring methods are usually associated with various degradation phenomenon like noise. Sophisticated imaging techniques like PET (Positron Emission Tomography) and SPECT (Single Photon Emission Computed Tomography) are two methods to obtain images non-invasively from the interior of a patient which extensively use restoration schemes to improve resolution in order to perform better diagnosis. Other than this it also finds its utility in Magnetic Resonance Imaging (MRI) [12]. Digital image

restoration techniques can contribute significantly for this [13].

Films reflects the culture from which it is stemmed and records our history, represent contemporary culture and have great artistic value. Thus, they are precious cultural assets which must be preserved. Unfortunately, because of aging, improper storage conditions and other reasons, old films are threaten with defects caused by decaying, dust, dirt, scratch and mold [14]. Consequently, digital film restoration, repairing defects in films, has been recognized as an important issue by archives, content owners and film companies. Motion picture restoration is not limited to eliminate scratches and dust from old movies, but also to colorize black-and-white films like Mughal-e-Azam. Only a small subset of the vast amount of work being done in this area can be classified under the category of image restoration. Much of this work belongs to the field of computer graphics and enhancement. Nonetheless, some very important work has been done recently in the area of digital restoration of films. Digital restoration of the film "Snow White"and the "Seven Dwarfs"by Walt Disney, which originally premiered in 1937 [15] are few to cite.

Image restoration has also received some notoriety in the media, and particularly in the movies of the last decades. The climax of the 1987 movie "No Way Out"was based on the digital restoration of a blurry Polaroid negative image [16]. The 1991 movie "JFK"made substantial use of a version of the famous Zapruder 8mm film of the assassination of the US President John F. Kennedy. It is no surprise that digital image restoration has been used in law enforcement and forensic science for a number of years. Complex problems like solving a crime often requires security video tapes, blurry photographs of license plates and crime scenes to be properly visualized for proper investigation. Image restoration helps in improving the quality of such images which are often needed when such photographs can provide the only link for solving a crime. Clearly, law enforcement agencies all over the world have made, and continue to make use of digital image restoration ideas in many forms.

Image and video coding is one of the exciting applications of image restora-

tion. Even though coding efficiency has improved and bit rates of coded images have reduced, there is another problem of blocking artifacts which needs significant improvement. These are as a result of the coarse quantization of transform coefficients used in typical image and video compression techniques. Usually, a Discrete Cosine Transform (DCT) will be applied to prediction errors on blocks of 8×8 pixels. Intensity transitions between these blocks become more and more apparent when the high-frequency data is eliminated due to heavy quantization. Already, much has been accomplished to model these types of artifacts, and develop ways of restoring coded images as a post-processing step to be performed after decompression [17–19].

Digital image restoration is being used in many other applications as well. Just to name a few, restoration has been used to restore blurry X-ray images of aircraft wings to improve aviation inspection procedures. It is used for restoring the motion induced effects present in still composite frames, and, more generally, for restoring uniformly blurred television pictures. Printing applications often require the use of restoration to ensure that halftone reproductions of continuous images are of high quality. In addition, restoration can improve the quality of continuous images generated from halftone images. Digital restoration is also used to restore images of electronic piece parts taken in assembly-line manufacturing environments. Many defense-oriented applications require restoration, such as that of guided missiles, which may obtained distorted images due to the effects of pressure differences around a camera mounted on the missile. All in all, it is clear that there is a very real and important place for image restoration technology today.

Image restoration is distinct from image enhancement techniques, which are designed to manipulate an image in order to produce results more pleasing to an observer, without making use of any particular degradation models. Image enhancement refers to the techniques by which we try to improve an image such that it looks subjectively better by improving the visual appearance of the image. On the other hand restoration emphasizes on getting back the original image as far as possible from the degraded one. Thus the goal of image enhancement is

very different from that of restoration. Better representation of image is obtained through image enhancement techniques, however, it would not be possible to define what enhancement exactly means, as an enhancement to one may be a noise to another [20]. Applying image enhancement scheme is of no use if the image which we want to enhance is of low quality or is degraded due to presence of noise or is an blurred image. So cascading schemes combining image noise removal followed by enhancement is among one of the solution for better visual perception. In this thesis we use such restoration techniques such that it can be used as a preprocessing step for enhancement producing better quality images.

Image reconstruction techniques operate on a set of image projections and not on a full image. Restoration and reconstruction techniques do share the same objective, however, which is that of recovering the original image, and they end up solving the same mathematical problem, which is that of finding a solution to a set of linear or nonlinear equations.

Digital image restoration is a field of engineering that studies methods used to recover an original scene from degraded observations. Developing techniques to perform the image restoration task requires the use of models not only for the degradations, but also for the images themselves. Image restoration problem is a subset of Inverse Problem. In general, in inverse problems, the values of a certain set of functions are estimated from the known properties of other functions. Consider the following relationship

$$\mathrm{L}(\{f_i\}, \{g_j\}) = 0 \tag{1.6}$$

where L is an operator, the function, $\{f_i\}$, are sought, and the values of the functions, $\{g_j\}$, are known. When the problem is well posed, the existence of solution is assured. Also there exists a unique solution for a given problem. However, in the presence of noise, the uniqueness of solution is not assured.

The image degradation and subsequent restoration may be depicted as in Figure 1.2(a). In this thesis, however, only noise part of entire degradation is dealt with, which is shown in Figure 1.2(b). We consider such noise removal schemes such that the output can be useful for further image enhancement while preserv-

ing image details during noise removal process. The following section provides a broad classification of restoration filters.

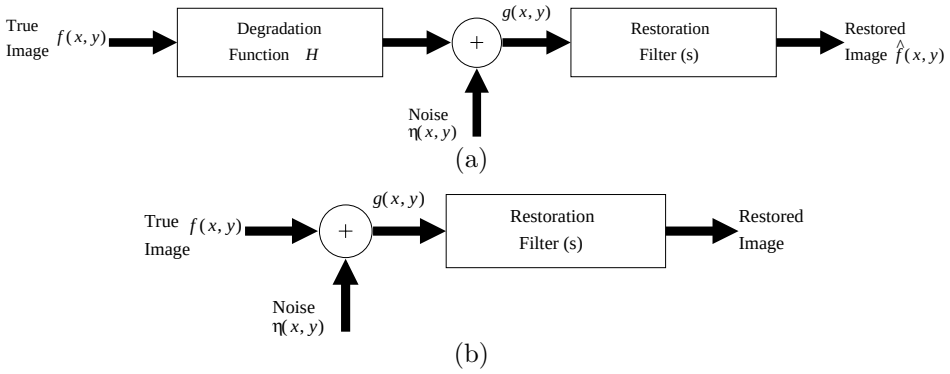

Figure 1.2: (a) Model of the image degradation/restoration process, (b) Model of the Noise Removal Process.

1.3 Filters

Image restoration, usually, employs different filtering techniques. Filtering may be done either in *spatial domain* or in *frequency domain*. In this thesis different spatial domain filtering techniques have been studied and proposed. Broadly, filters may be classified into two categories: *Linear* and *Nonlinear*. The filtering methodologies are described below.

1.3.1 Linear Filters

In the early development of image processing, linear filters were the primary tools. Their mathematical simplicity with satisfactory performance in many applications made them easy to design and implement. However, in the presence of noise the performance of linear filters is poor. In image processing applications they tend to blur edges, do not remove impulsive noise effectively, and do not perform well in the presence of signal dependent noise [21].

Mathematically, a filter may be defined as an operator $L(\cdot)$, which maps a signal x into a signal y:

$$y = L(x) \tag{1.7}$$

When the operator $L(\cdot)$ satisfies both the superposition and proportionality principles, the filter is said to be linear. Two-dimensional and m-dimensional linear

filtering is concerned with the extension of one-dimensional filtering techniques to two and more dimensions. If impulse response of a filter has only finite number of non-zero values, the filter is called a *finite impulse response* (FIR) filter. Otherwise, it is an *infinite impulse response* (IIR) filter [22].

If the filter evaluates the output image only with the input image, the filter is called *non-recursive*. On the other hand, if the evaluation process requires input image samples together with output image samples, it is called *recursive* filter [4, 21, 23]. Following are the few main types of filters:

- *Low-pass filter*: Smooths the image, reducing high spatial frequency noise components.
- *High-pass filter*: Enhances very low contrast features, when superimposed on a very dark or very light background.
- *Band-pass filter*: Tends to sharpen the edges and enhance the small details of the image.

1.3.2 Nonlinear Filters

Nonlinear filters also follow the same mathematical formulation as in (1.7). However, the operator $L(\cdot)$ is not linear in this case. Convolution of the input with its impulse response does not generate the output of a nonlinear filter. This is because of the non-satisfaction of the superposition or proportionality principles or both [21–23].

Gray scale transformations [1, 3, 6] are the simplest possible nonlinear transformations of the form (1.7). This corresponds to a memory less nonlinearity that maps the signal x to y. The transformation

$$y = t(x) \tag{1.8}$$

may be used to transform one gray scale x to another y. This type of gray level transform are extensively used for enhancing the subjective quality of the images as per the need of the application. *Histogram modification* is another form of

intensity mapping where the relative frequency of gray level occurrence in the image is depicted. An image may be given a specified histogram by transforming the gray level of the image into another. *Histogram equalization* is one such methods that is used for this purpose. The need for it arises when comparing two images taken under different lighting conditions. The two images must be referred to the same base, if meaningful comparisons are to be made. The base that is used as standard has a uniformly distributed histogram [1, 3, 6]. Of course, a uniform histogram signifies maximum information content of the image [24]. Histogram based approaches as discussed above are used as simple image enhancement techniques in various applications. Figure 1.3 gives a graphical representation of the various families of nonlinear filters [21].

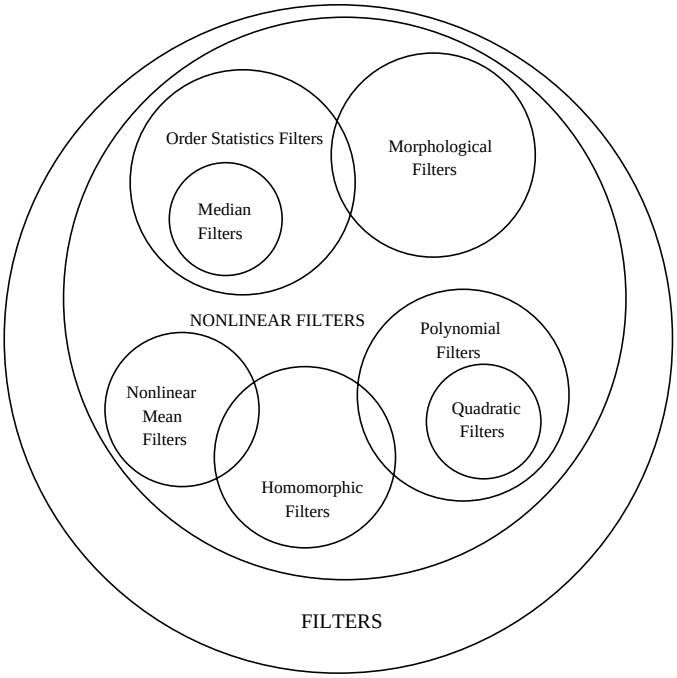

Figure 1.3: Nonlinear Filter Family

Order statistic filters [21, 23] for noise removal are the most popular class nonlinear filters. A number of filters belongs to this class of filters, e.g., the median filter, the stack filter, the median hybrid filter etc. Nonlinear filters based on order statistics have excellent robustness properties in the presence of impulsive noise. They tend to preserve edge information, which is very important for human perception. Even there computation is relatively easy and fast as compared to some

linear filters. Such properties of those filters have created numerous applications in digital image processing.

There exists some approaches that utilizes geometric features of signals rather than analytic features of signals. Their origin is basic set operations for image processing. These filters are called morphological filters and find applications in image processing and analysis. Biomedical image processing, shape recognition, edge detection, image enhancement are few other areas, where it is used extensively [1, 3, 6, 21, 23].

One of the oldest class of nonlinear filters, which have been used extensively in digital signal and image processing, are homomorphic filters and their extensions. These filter class find its applications in image enhancement, multiplicative and signal dependent noise removal, speech processing and also in seismic signal processing [1, 3, 6, 21, 23].

Adaptive filtering has also taken advantage of nonlinear filtering techniques. Non-adaptive nonlinear filters are usually optimized for a specific type of noise and signal. When, however, the filter is required to operate in an environment of unknown statistics or a non stationary environment, an adaptive filter provides an elegant solution to this more difficult problem. Images can be modeled as two-dimensional stochastic processes, whose statistics vary in the various image regions and also from applications to applications. In such situations, adaptive filters become the natural choice and their performance depends on the accuracy of estimation of certain signal and noise statistics [1, 3, 6, 21, 23]. The filter starts from an arbitrary initial condition, knowing nothing about the environment, and proceeds gradually towards an optimal solution.

Considerable attenuation has been given nonlinear estimation of signals corrupted with noise. Despite impressive growth in last few decades, nonlinear filtering techniques still lack a unifying theory that encompasses existing nonlinear processing techniques.

1.4 Problem Definition

Different types of noise frequently contaminate images. Impulsive noise is one such noise, which may affect images at the time of acquisition due to noisy sensors or at the time of transmission due to channel errors or in storage media due to faulty hardware. Two types of impulsive noise models are described below.

Let $Y_{i,j}$ be the gray level of an original image Y at pixel location (i, j) and $[n_{min}, n_{max}]$ be the dynamic range of Y. Let $X_{i,j}$ be the gray level of the noisy image X at pixel (i, j) location. *Impulsive Noise* may then be defined as:

$$X_{i,j} = \begin{cases} Y_{i,j} & \text{with } 1-p \\ R_{i,j} & \text{with } p \end{cases} \tag{1.9}$$

where, $R_{i,j}$ is the substitute for the original gray scale value at the pixel location (i, j). When $R_{i,j} \in [n_{min}, n_{max}]$, the image is said to be corrupted with *Random Valued Impulsive Noise* (RVIN) and when $R_{i,j} \in \{n_{min}, n_{max}\}$, it is known as *Fixed Valued Impulsive Noise* or *Salt & Pepper Noise* (SPN).

The difference between SPN and RVIN may be best described by Figure 1.4. In the case of SPN the pixel substitute in the form of noise may be either $n_{min}(0)$ or $n_{max}(255)$. Where as in RVIN situation it may range from n_{min} to n_{max}. Cleaning such noise is far more difficult than cleaning fixed-valued impulse noise since for the latter, the differences in gray levels between a noisy pixel and its noise-free neighbors are significant most of the times. In this thesis, we focus only on *random valued impulse noise* (RVIN) and schemes are proposed to suppress RVIN.

One common drawback of typical image sharpening (enhancement) methods is that they tend to boost noise while amplifying the image details making the image more noisy. This undesirable amplification limits the real time applications of sharpening algorithms. Typical solution to deal with noise amplification when performing enhancement is perform noise reduction prior to enhancement. However, noise filters not only suppress noise but also tend to blur the image details producing low quality images [25]. This is because noise reduction is commonly a low pass filtering operation, whereas sharpening is a high-pass operation. Hence, there is a conflicting spectral demand on both filters, and generally, the optimiza-

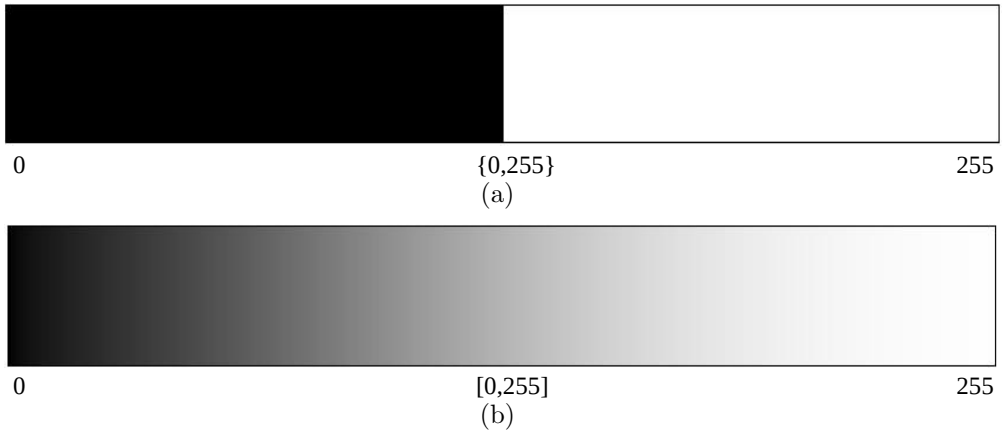

Figure 1.4: Representation of (a) *Salt & Pepper Noise* with $R_{i,j} \in \{n_{min}, n_{max}\}$, (b) *Random Valued Impulsive Noise* with $R_{i,j} \in [n_{min}, n_{max}]$

tion of one leads to deterioration of the other [26].

1.5 Performance Measures

The metrics used for performance comparison of different filters (exists and proposed) are defined below.

a. Peak Signal to Noise Ratio ($PSNR$)

$PSNR$ analysis uses a standard mathematical model to measure an objective difference between two images. It estimates the quality of a reconstructed image with respect to an original image. The basic idea is to compute a single number that reflects the quality of the reconstructed image. Reconstructed images with higher PSNR are judged better. Given an original image Y of size $(M \times N)$ pixels and a reconstructed image $\hat{Y}$, the $PSNR(dB)$ is defined as:

$$PSNR(dB) = 10 \log_{10} \left(\frac{255^2}{\frac{1}{M \times N} \sum_{i=1}^{M} \sum_{j=1}^{N} \left(Y_{i,j} - \hat{Y}_{i,j} \right)^2} \right) \tag{1.10}$$

b. Percentage of Spoiled Pixels (PSP)

PSP is a measure of percentage of non-noisy pixels change their gray scale values in the reconstructed image. In other words it measures the efficiency

of noise detectors. Hence, lower the PSP value better is the detection, in turn better is the filter performance.

$$PSP = \frac{\text{number of non-noisy pixels changed their gray value}}{\text{total number of non-noisy pixels}} \times 100 \quad (1.11)$$

c. Subjective or Qualitative measure

Along with the above performance measure subjective assessment is also required to measure the image quality. Unavailability of quantitative performance measure in case of image enhancement (sharpening) subjective or qualitative measure is the only option left for measurement [27]. In a subjective assessment measures characteristics of human perception become paramount, and image quality is correlated with the preference of an observer or the performance of an operator for some specific task. Hence as an usual case of image enhancement there is no quantitative performance evaluation measure because no ideal image can be used as reference. Any reasonable measure should be tuned to the human visual system. However perceptual quality evaluation is not a deterministic process. So subjective evaluation is the only way to prove the performance. Hence human observer is the only way by which enhanced image quality can be measured. All the proposed schemes are hence compared with the subjective results of well accepted schemes.

In the thesis, Chapter 5 deals with image sharpening (enhancement) under noisy conditions and no reference ideal image is available for comparison of objective indices. In such a situation the subjective measure is the only alternative to be used.

1.6 Literature Survey

In this section literature survey is presented under two heads noise removal and prevention of noise boosting in contrast enhancement. Noise removal from a contaminated image signal is still a challenging problem for researchers. Many researchers have suggested a large number of algorithms and compared their results.

The main thrust on all such algorithms is to remove impulsive noise while preserving image details. These schemes differ in their basic methodologies applied to suppress noise. Some schemes utilize detection of impulsive noise followed by filtering whereas others filter all the pixels irrespective of corruption. In this section an attempt has been made for a detail literature review on the reported articles and study their performances through computer simulation. We have classified the schemes based on the characteristics of the filtering schemes and described are below. We also describe some of the conventional contrast enhancement techniques in this section, boosting in images can be prevented with proper

1.6.1 Impulsive Noise Removal

A. Filtering without Detection

In this type of filtering a window mask is moved across the observed image. The mask is usually of size $(2N+1)^2$, where N is a positive integer. Generally the center element is the pixel of interest. When the mask is moved starting from the left-top corner of the image to the right-bottom corner, it performs some arithmetical operations without discriminating any pixel.

B. Detection followed by Filtering

This type of filtering involves two steps. In first step it identifies noisy pixels and in second step it filters those pixels. Here also a mask is moved across the image and some arithmetical operations is carried out to detect the noisy pixels. Then filtering operation is performed only on those pixels which are found to be noisy in the previous step, keeping the non-noisy intact.

C. Hybrid Filtering

In such filtering schemes, two or more filters are suggested to filter a corrupted location. The decision to apply a particular filter is based on the noise level at the test pixel location or performance of the filter on a filtering mask.

All those filtering schemes that are reviewed are described in this section under their respective head.

A. Filtering without Detection

As discussed in the previous section, this technique does not detect contaminated pixels. It applies the filtering mechanism through out the subject without discriminating any pixel.

A1. Moving Average [3]

This is a simple linear filter. Average of all pixels of a sliding window is replaced with the pixel of interest.

$$\hat{Y}_{i,j} = \frac{1}{m \times n} \sum_{(u,v) \in S_{mn}} X_{u,v} \tag{1.12}$$

where, X is the noisy image, $\hat{Y}$ is the restored image and S_{mn} is the sliding window of size $m \times n$ centered around (i, j). Its performance both in subjective as well as objective way is very poor.

A2. Median (3×3) A3. Median (5×5) [3]

The median filter (1.13) is one of the most popular nonlinear filters. It is very simple to implement and much efficient as well. But the cost is that it blurs the image and edges are not preserved. It acts like a low pass filter which blocks all high frequency components of the image like edges and noise, thus blurs the image.

$$\hat{Y}_{i,j} = \text{MEDIAN}_{(u,v) \in S_{mn}} \left(X_{u,v} \right) \tag{1.13}$$

Depending upon the sliding window mask there may be many variations of median filter. Here we have reviewed two such variations. Median (3×3) filter makes use of a 3×3 sliding window, whose center pixel is replaced with the median value of all the 9 pixels of the window. This kind of filter is helpful when noise is scattered throughout the image. Whereas median (5×5) filter replaces the pixel of interest i.e. the center pixel with the median value of all the 25 pixels of the sliding window. When noise appears in blotch, this type of filter works better. But for other situations it produces disappointing results.

A4. WM[1] $k = 1$ **A5. WM $k = 2$ [28–31]**

This is another nonlinear median filter, which favors the center pixel than others. Let the window size be $(2n+1)^2$ and $L = 2n(n+1)$. The filter is defined as:

$$\hat{Y}_{i,j}^{2k} = \text{MEDIAN}\{X_{i-u,j-v}, (2k) \diamond X_{i,j} | -h \leq u, v \leq h\} \tag{1.14}$$

where $2k$ is the weight given to pixel (i, j), and $\diamond$ represents the repetition operation. Hence in a 3×3 window $\hat{Y}_{i,j}^{2k}$ is the median of $(9 + 2k)$ gray values with the center value of the window repeated $(2k + 1)$ times. $\hat{Y}_{i,j}^{0}$ is the standard median filter, where as $\hat{Y}_{i,j}^{2k}$ becomes identity filter when $k \geq L$. Two variations of WM (with $k = 1$ and $k = 2$) have been simulated. When the noise percentage is low, both the filters work better but beyond 10% of noise the performance starts deteriorating. If noise appears as blotch in a window, it leaves the blotch as it is as if no filtering has been done.

B. Detection followed by Filtering

Such filtering schemes differentiate between noisy and non-noisy pixels. These filters, in general, consist of two steps. Detection of noisy pixels is followed by filtering. Filtering mechanism is applied only to the noisy pixels.

B1. Rank-Ordered Mean [32]

This is an adaptive approach to solve the restoration problem in which filtering is conditioned on the current state of the algorithm. The state variable is defined as the output of a classifier that acts on the differences between the current pixel value and the remaining ordered pixel values inside a window centered around the pixel of interest.

This scheme is undoubtedly one of the robust and simple scheme but it fails in preserving the finer details of the image.

B2. Progressive-Switching Median [33]

It is a median based filter, which works in two stages. In the first stage an impulse detection algorithm is used to generate a sequence of binary flag images. This

[1]WM: Weighted Median

binary flag image predicts the location of noise in the observed image. In the second stage noise filtering is applied progressively through several iterations.

This filter is a very good filter for fixed valued impulsive noise but for random values the performance is abysmal.

B3. Adaptive Center Weighted Median Filter [29]

This work is an improvement of previously described Center Weighted Median (CWM) filter. It works on the estimates based on the differences between the current pixel and the outputs of the CWM filters with varied center weights. These estimates decide the switching between the current pixel and median of the window.

This is a good filter and is robust for a wide variety of images. But it is inefficient in recovering the exact values of the corrupted pixels.

As the name suggests it employs median filter on the noisy image twice. This adaptive system tries to correct for false replacements generated by the first round of median filtering operation. Based on the estimated distribution of the noise, some pixels changed by first median filter are replaced by their original values and kept unchanged in the second median filtering. And in the second round it filters out the remaining impulses.

Even though the filter gives some good results in terms of noise suppression but spoiling of good pixels is more and it results in overall poor performance.

B5. Accurate Noise Detector [34]

This filter justifies its name by detecting noise to the perfection. Based on Progressive Switching Median Filter, it generates an edge flag image to classify the pixels of noisy image into ones in the flat regions and edge regions. The two types of pixels are processed by different noise detector. When noise is very high prevention of false-detection and non-detection becomes difficult. Therefore, another iteration is dedicated for verification of the noise flag image.

This scheme exhibits good performance on images not only with low noise density but also with high percentage of corruption. But all these come at the

cost of computational complexity which is very high and not at all suitable for real time applications.

B6. SM[2] (5×5) B7. SM (7×7) B8. SM (9×9) [35]

This is also a two stage process, where in the first stage noise detection is carried out and in the second stage filtering is done. The noisy image is convolved with a set of convolution kernels. Each of the kernels are sensitive to edges in a different orientation. The minimum absolute value of these four convolutions is used for impulse detection by comparing with a threshold. By varying the size of kernel different variations of SM may be obtained. Three such variations of SM are reviewed here in this paper.

Because of its four kernels it detects noise effectively even in those images where the edge density is more. But when the kernel size increases to 7×7 and 9×9 it fails in doing so. Also it fails in preserving finer details.

B9. Differential Ranked Impulse Detector [36]

This is another nonlinear technique which also works in two stages. It aims at filtering only corrupted pixels. Identification of such pixels is done by comparing signal samples within a narrow rank window by both rank and absolute value. The first estimate is based on the comparison between the rank of the pixel of interest and rank of the median. The second estimate is based on the brightness value which is analyzed using the median.

It is a good filter in low noise conditions but the performance slightly degrades in beyond 20% of noise. It also leaves noise blotch without correcting.

B10. Enhanced Ranked Impulse Detector [36]

This scheme is an alteration of the scheme described above. Here the brightness is analyzed by calculating the difference of pixel of interest with its closest neighbors in the variational series.

Its performance is very good at low noise but fails miserably at noise density more than 20%.

[2]SM: Switching Median

B11. Advanced Impulse Detection Based on Pixel-Wise MAD [37]

This scheme is based on modified median of absolute deviation from median (MAD). MAD is used to estimate the presence of image details. An iterative pixel wise modification of MAD is used here that provides a reliable removal of impulses. Its performance is more than average and fails when the edge density is more.

B12. Minimum-Maximum Exclusive Mean [38]

This is a simple nonlinear, robust filter that centers around two windows of size 3×3 and 5×5. It checks for a particular range of gray level in the 3×3 windows. If it fails it goes to 5×5 window. If average of all the pixels of that particular range is more than certain value then that pixel is replaced with the average, otherwise it is left intact. This is one of the good schemes because of its simplicity and easy implementation.

B13. Peak and Valley [39]

This recursive nonlinear filter is composed of two conditional rules. It compares the test pixel with surrounding neighbor pixels for some conditions. It then replaces the pixel of interest with the most conservative surrounding pixel. This scheme is computationally efficient over others but at the same time it spoils non-noisy pixels to a greater extent.

B14. Detail preserving impulsive noise removal [40]

Unlike thresholding techniques, it detects noisy pixels non-iteratively using the surrounding pixel values. It is based on a recursive minimum maximum method of Peak and Vally scheme. When the image contains numerous edges like *Babbon*,*Clown* etc. this technique totally fails.

B15. Signal-Dependent Rank Ordered Mean [41]

This is one of the most efficient nonlinear algorithms to suppress impulsive noise from highly corrupted images. Based on detection-estimation strategy, this algorithm replaces the identified noisy pixel with rank ordered mean of it surroundings.

C. Combined Filtering

Two or more filters are employed in this type of filtering mechanism. In addition to this a switch is used whose logic helps in switching among the employed filters. The switch may take output of individual filter into consideration or by some other means to decide which filter should be employed for a particular window such that the final output would be the best.

C1. Tri-State Median Filtering [42]

This combined filter comprises of standard median filter, identity filter, center weighted median filter and a switching logic. Noise detection is realized by an impulse detector, which takes the outputs from the standard median and center weighted median filters and compares them with the center pixel value in order to make a tri-state decision. The switching logic is controlled by a threshold value. Depending on this threshold value, the center pixel value is replaced by the output of either SM filter or CWM filter or identity filter. This is one of the good schemes reviewed in this paper.

C2. Two-Output Filter [43]

The two-output nonlinear filter is based on the subsequent activation of two recursive filtering algorithms that operates on different subsets of input data. One subset is the right-bottom 3×3 sub-window and the other one is left-top 3×3 sub-windows of a 4×4 sliding window. Two center pixels of both 3×3 sub-windows are updated at each step. Rank ordered filtering is used to remove impulsive noise. This is a good scheme and gives very good result under fixed valued impulsive noise conditions. But under random valued impulsive noise it fails miserably.

C3. MRHF[3]-1 C4. MRHF-2 C5. MRHF-3 [44]

This is a class of non-linear filters called Median Rational Hybrid Filters based on a rational function. The filter output is the result of a rational operation taking into account three sub function. In all the three operations the central operation

[3]MRHF: Median Rational Hybrid Filter

is CWM.

In MRHF-1 the CWM gives ϕ_2 and two FIR sub filters give ϕ_1 and ϕ_3. The rational function on ϕ_1, ϕ_2 and ϕ_3 decides which of the filter is most suitable.

In MRHF-2 the sub-filters are four unidirectional median filters. Mean of two median filters gives ϕ_1 and mean of other two gives ϕ_3. And the CWM gives ϕ_2. The rational function decides based on these three ϕ values.

In MRHF-3 two bidirectional median filter give ϕ_1 and ϕ_3. Together with ϕ_2 from CWM the rational function takes the decision.

Spoiling of non-noisy pixels is high in all the three filters. When compared among the three, the MRHF-2 outperforms other two.

1.6.2 Prevention of Noise Amplification in Image Sharpening

Loss of sharpness can be caused by poor resolution of the imaging device, limited transmission bandwidth, reflections or echoes in the channel, or poor display. These anomalies can be improved upon by applying image enhancement techniques. The techniques to achieve enhancement usually separate the high and/ or low frequency components of the image, manipulating them separately and recombine them together with desired weights. The UM or the high frequency emphasizing methods which belongs to this category faces a severe drawback that is noise amplification. Applying those schemes to low contrast noisy images produces undesirable artifacts resulting low quality images. These artifacts become too strong in particularly in dark regions resulting visually less pleasing enhanced images. Performance of UM is improved using non linear filters like quadratic filters [45], Volterra filters [45], morphology based nonlinear filters [46] instead of linear high pass filters. In an alternate approach the amplification factor is estimated recursively by considering the statistics of neighboring pixel values. Adaptive Unsharp Masking [47] controls the contributions of the amplification factor in such a way that image enhancement occurs in high detail areas and little or no image sharpening occurs in smooth areas. Another solution for noise amplification is cascading of noise filters with UM. This scheme does not gives the best

performance always. Since noise filters tend to blur image details, while UM tend to increase noise so spectrally this arrangement cannot produce an optimal result. There is a conflicting spectral demand on both hence optimization of one leads to deterioration of the other. Little variation of this approach is noise filtering after UM, this is seldom preferred because the noise filter will remove the sharpness enhancement created by UM [5]. So noise filtering followed by UM is a simple enhancement method, but proper filter must be chosen so that it preserves image details while filtering noise. Hence, proper compromise between image smoothing (noise removal) and sharpening must be done to obtain an image for better perception.

Procedures for sharpening images under noisy conditions can be classified under two heads:

α. Integrated Noise Reduction and Sharpness Enhancement

β. Cascaded Noise Reduction and Sharpness Enhancement

α. Integrated Noise Reduction and Sharpness Enhancement

Under this category no specialized filter or method is applied to remove noise before UM. In this approach importance is given to noise sensitivity or to avoid such image regions which may be noisy.

α1. Quadratic Filter [25]

Quadratic filters are the simplest non linear time-invariant systems and correspond to the second term of the Volterra expansion [48]. Such filters are completely defined by their kernel which is a symmetric finite of infinite square matrix. Inspite of their nonlinear properties they behave like linear high pass filter. One of them can be formulated as [49]:

$$H_{i,j} = 4\hat{I_{i,j}} - \hat{I_{i-1,j}} - \hat{I_{i+1,j}} - \hat{Y_{i,j-1}} - \hat{I_{i,j+1}} \tag{1.15}$$

Using these filters in UM may still introduce some visible noise, depending on the amplification factor. To have better performance the output of high pass filter can be multiplied by a control signal obtained from an edge sensor.

α2. Normalized Nonlinear UM [50]

This is an alternate approach to reduce the noise effects and to modify the UM structure by replacing the sharpening components of simple linear UM scheme by an enhancement fraction derived from quadratic filters.

α3. Adaptive UM [51]

In this new approach sharpening action is performed only in locations where the image exhibits significant dynamics. Hence, the amplification of noise in smooth areas is reduced. All this is achieved by proper tuning of amplification factor λ. In the previous schemes the factor λ was fixed for the whole image. In adaptive UM, the factor λ is controlled by values of the pixels in a neighborhood. Low contrast details are much more enhanced than the high contrast details in adaptive UM.

β. Cascaded Noise Reduction and Sharpness Enhancement

Cascaded noise reduction and sharpness enhancement algorithms have been implemented to have images of high quality for human as well as machine perception. This combination of smoothing and sharpening is achieved by using noise filters along with UM [11,52]. The type of filter to be used depends on the allowed noise level of the output image. The complete cascaded scheme can be narrated as filtering out impulse noise (smoothing) and sharpening image details. Noise smoothing and edge enhancement are inherently conflicting processes, since smoothing a region might destroy an edge and sharpening may lead to unnecessary noise amplification. A plethora of such techniques have been proposed in the literature [53,54]. Common filters used here to reduce impulse noise belongs to the category filtering without detection, because of there simplicity. It can be easily realized from the previous schemes that noise removal is very important before image enhancement. Slight amount of noise can even degrade the quality of an image drastically after enhancement. In this section, we discuss those techniques which uses a particular filter to remove noise followed by UM. The performance of cascading algorithms depend mostly on the filtering scheme. The objective is to preserve the image details while filtering noise so that enhancement algorithms can enhance the images

properly. As per the review under the section impulse noise removal it is observed that detection followed by filtering scheme is the best. So as per this we can have different combination of filters with well known unsharp masking. The quality of enhancement will depend upon the amount of noise removed by the filter. Few combinations of simple filtering schemes along with UM is discussed below.

β1. Median Filtering followed by Unsharp Masking [45]

All the steps of unsharp masking remains same except a non linear median filter [3] output is used as the input to the unsharp masking stage. This filter is able to remove noise up to some extent but it also blurs the edges since filtering is applied to all the pixels. Since the image details are lost while filtering the enhanced images are not satisfactory and it only works under low noise condition.

β2. Weighted Median Filtering followed by Unsharp Masking [55]

There have been several variations on the median filter, for example the weighted median filter [30, 56] selectively gives the neighboring pixels multiple entries to the ordered list, usually with the center pixels of the neighborhood contributing more entries. this performance is better in higher noise conditions. The higher the weighting given to the central pixel, the better the filter is at preserving corners, but the less the smoothing effect is. So its output can be used for getting enhanced images using UM but not in high noise conditions.

β3. PWMAD Filtering followed by Unsharp Masking

As an alternate to median filtering and its variations an advanced selective filtering scheme is applied along with UM. PWMAD [37] is based on modified median of absolute deviation from median (MAD). Its performance in filtering and hence with UM is more than average and the filtering fails when the edge density is more.

1.6.3 Simulation of Existing schemes, Results and Discussion

Lena image corrupted with RVIN (1% to 30% of noise) is subjected to the different filtering schemes discussed above and their performance is measured using metrics (1.10) and (1.11). Table-1.1 lists the $PSNR$ where as Table-1.2 lists the PSP of different filters. Figures 1.5– 1.7 depict the performance of each scheme in their respective groups.

The performance in $PSNR$ of Group-A schemes is depicted in Figure 1.5. The performance of A1 is very poor in comparison to others. A3's performance is steady, which is around $30dB$. A5 is in commanding position at very low noise density but flunks at other situations. A2 is better in the upper half where as A4 is better in the lower half of noise density.

Group-B performance is depicted in Figure 1.6. B15 is one of the filters that outperforms rest all. When comparing other schemes it can be seen that, in the very low noise density (around 1%) B6 and B9 outperforms all others. When the density increases (low noise, 5%–15%) B3, B4, B10 and B11 performs equally good but B6 and B9 decline drastically. When the density further increases (medium noise, 20%–30%), all the schemes perform more or less same. But B3 and B4 are slightly better than others in this range of noise.

Figure 1.7 unequivocally depicts that C1 is not only the winner in Group-C but also outperforms all other schemes in the same group. Performances of C3, C4 and C5 are almost same where as C2 produces very poor results.

Some of the schemes, whose performance is better in SPN model of noise are also compared. Figure 1.11 shows the PSNR (dB) variations and Figure 1.12 PSPs of such schemes.

However, an inherent difficulty in image sharpening or enhancement is unavailability of mathematical criterion for visual quality. As a result final assessment can only be performed by human observer. Subjective evaluation of Image Sharpening is depicted in Figure 1.13. Subjective evaluation of the images in Figure 1.13 shows that $\beta 3$ has better performance in comparison to $\alpha 1$, $\alpha 2$, $\beta 1$ and $\beta 2$ under noisy conditions.

1.7 Motivation

In the literature, for suppression of impulsive noise mostly the filtering schemes fall under two categories. First, filtering without detection of noise, where as the second category filters apply detection mechanism [29, 34–37, 40, 41, 43, 44, 57, 58]. The later schemes are superior to former ones in terms of noise rejection as well as retention of edges in restored images. It is also observed the performance of any filtering scheme is dependent on the detection mechanism. The better is the detector, the superior is the filtering performance. Hence the performance of a detector plays a vital role. In turn, the detector performance is solely dependent on a threshold value which is compared with aprecomputed numerical value. Mostly the reported schemes use a fixed threshold which do not serve the purpose at various noise conditions as well as in different images. Hence to improve the detector performance need for an adaptive threshold is an utmost necessity which can be automatically determined from the charecterstics of an image and the noise present in it. In this thesis, attemts have been made to determine an threshold from an observed noisy image. This problem has been formulated as an prediction problem and various neural network models have been chosen as tools based on statistical parameters derived from the input noisy images.

In summary, the thesis objectives is listed as:

- to use better image statistics for identifying contaminated pixels and decrease computational complexity.
- to work towards improved and efficient detectors for identifying contaminated pixels using different neural detectors.
- to devise adaptive thresholding techniques so that noise detection would be more reliable.
- to explore the utilities of selective filtering to image sharpening to produce high quality images with preserved image details.

1.8 Thesis Organization

The rest of the thesis is organized as follows.

Chapter 2 proposes restoration schemes for images contaminated with *Random Valued Impulsive Noise*. The proposed schemes are based on second order difference of pixels. An adaptive threshold value is used to determine the noise status of each pixel. Mean and variance are used to train the neural detectors. Three different ways of selecting the threshold value are presented. The first approach uses an *Multilayer Perceptron* network trained with back propagation algorithm to detect noisy pixels. The second approach uses an *Functional Link Artificial Neural Network* to determine the noise threshold. And the last scheme uses a *Radial Basis Functional Network* to estimate the sanctity of a test pixel. Comparative analysis with most recent techniques reveal that the proposed techniques are better in terms of noise suppression.

In **Chapter 3** again we use a Functional Link Artificial Neural Network to determine the threshold with reduced input parameters. Emphasis is given on the use of better image statistics for training the neural detector. A single parameter coefficient of variance (CV) of the noisy image is used in this scheme, which reduces the training time considerably and the noise detection becomes more accurate. Exhaustive simulations on different standard images and subsequent comparisons reveal that this proposed scheme outperforms existing schemes both qualitatively as well as quantitatively.

The objective of **Chapter 4** is to critically study the comparative filtering performance amongst the various methods proposed in this thesis. A conclusion has also been drawn to choose a method for impulse noise filtering under a particular noise situation.

Chapter 5 covers the topic image sharpening under impulsive noise condition. Prevention of noise amplification and image detail preservation in image sharpening schemes i.e. Unsharp Masking is achieved using selective

filtering. Subjective comparison of the proposed scheme resulted with well accepted result in comparison to existing schemes.

Finally **Chapter 6** presents the concluding remark, with scope for further research work.

1.9 Summary

The fundamentals of digital image processing, sources of noise and types of noise in an image, the existing filtering schemes and their merits and demerits and the various image metrics are studied in this chapter. Applications of neural architectures have been underutilized in the surveyed schemes. To derive the benefits of this paradigm, investigation has been made in this thesis to develop some novel schemes in the area of image restoration. Further applications of selective filtering to image enhancement is also been explored in this thesis.

Table 1.1: Comparative Results in PSNR (dB) of different filters for *Lena* image corrupted with RVIN of varying strengths

$Noise \Rightarrow$ / $Filters \Downarrow$	1%	5%	10%	15%	20%	25%	30%
A1	28.16	26.76	24.19	22.44	21.07	20.01	19.11
A2	35.04	33.96	32.81	31.65	30.25	28.94	27.39
A3	30.95	30.4	29.82	29.22	28.48	27.96	27.32
A4	38.19	36.11	33.99	31.76	29.32	27.30	25.25
A5	41.16	36.05	31.26	27.73	24.87	22.70	20.88
B1	31.64	31.01	30.25	29.60	28.86	28.15	27.39
B2	31.95	31.28	30.81	30.05	29.27	28.54	27.84
B3	36.08	34.77	33.37	32.21	31.12	29.02	28.02
B4	35.32	34.15	32.94	31.88	30.59	29.40	28.19
B5	31.51	30.33	29.03	28.23	27.18	26.59	25.84
B6	40.55	35.01	31.84	29.71	27.97	26.66	25.43
B7	33.9	31.86	30.3	29.01	27.57	26.59	25.60
B8	30.48	29.31	28.09	27.11	26.03	25.18	24.22
B9	42.08	36.01	32.12	28.89	26.40	24.35	22.68
B10	39.21	36.06	33.85	31.64	30.80	28.91	27.22
B11	37.10	35.47	33.55	31.72	29.52	27.34	25.39
B12	38.93	33.47	30.06	27.63	25.67	24.13	22.73
B13	35.99	34.68	32.89	30.93	28.36	26.48	24.35
B14	36.87	33.34	29.53	26.62	24.37	22.64	21.07
B15	42.90	38.68	35.80	33.95	32.24	30.90	29.63
C1	39.49	36.06	34.01	31.61	29.09	28.46	27.88
C2	31.92	24.92	21.97	20.21	18.91	17.95	17.06
C3	30.97	29.38	27.03	24.89	23.02	21.46	20.13
C4	32.01	30.24	27.73	25.47	23.50	21.84	20.42
C5	31.59	30.02	27.73	25.56	23.62	22.02	20.60

Table 1.2: Comparative Results in PSP of different filters for *Lena* image corrupted with RVIN of varying strengths

$Noise \Rightarrow$ / $Filters \Downarrow$	1%	5%	10%	15%	20%	25%	30%
A1	98.99	99.08	99.13	99.18	99.32	99.45	99.56
A2	66.71	67.4	68.12	68.45	69.14	69.63	69.97
A3	78.23	78.84	79.43	79.73	80.34	80.77	80.98
A4	40.58	40.28	39.7	39.34	38.99	38.67	38.27
A5	22.84	21.77	20.60	19.52	18.40	17.61	16.92
B1	96.85	97.03	97.25	97.39	97.53	97.78	97.96
B2	00.00	00.05	00.09	00.05	00.11	00.00	00.22
B3	06.36	06.70	07.06	07.55	07.89	08.57	09.38
B4	59.01	59.52	60.05	60.56	61.14	61.74	62.29
B5	00.00	00.00	00.02	00.05	00.08	00.06	00.00
B6	00.13	00.17	00.21	00.26	00.32	00.44	00.58
B7	01.27	01.49	01.62	01.96	02.29	02.88	03.37
B8	03.63	04.06	04.49	05.22	06.03	07.13	08.47
B9	00.09	00.09	00.1	00.12	00.12	00.16	00.17
B10	01.17	01.21	01.33	01.49	01.79	02.21	02.75
B11	08.70	08.81	08.90	09.05	09.20	09.50	10.08
B12	00.33	00.60	01.24	02.21	03.62	05.37	07.68
B13	51.46	51.86	52.31	52.71	53.43	53.85	54.41
B14	25.63	23.87	21.98	19.93	18.25	17.13	15.63
B15	0.28	0.28	0.33	0.32	0.34	0.40	0.47
C1	00.74	00.79	00.89	00.99	01.16	01.14	01.59
C2	00.01	00.03	00.05	00.06	00.09	00.09	00.13
C3	99.12	99.15	99.18	99.19	99.2	99.21	99.22
C4	92.79	93.34	93.87	94.39	94.99	95.34	95.87
C5	92.28	92.72	93.16	93.62	94.14	94.45	94.91

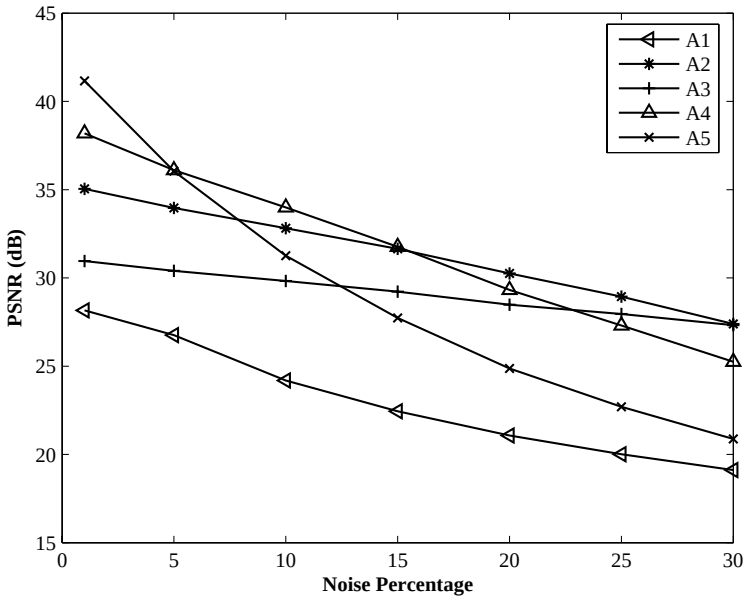

Figure 1.5: PSNR (dB) variations of *Lena* image corrupted with RVIN by Group-A schemes

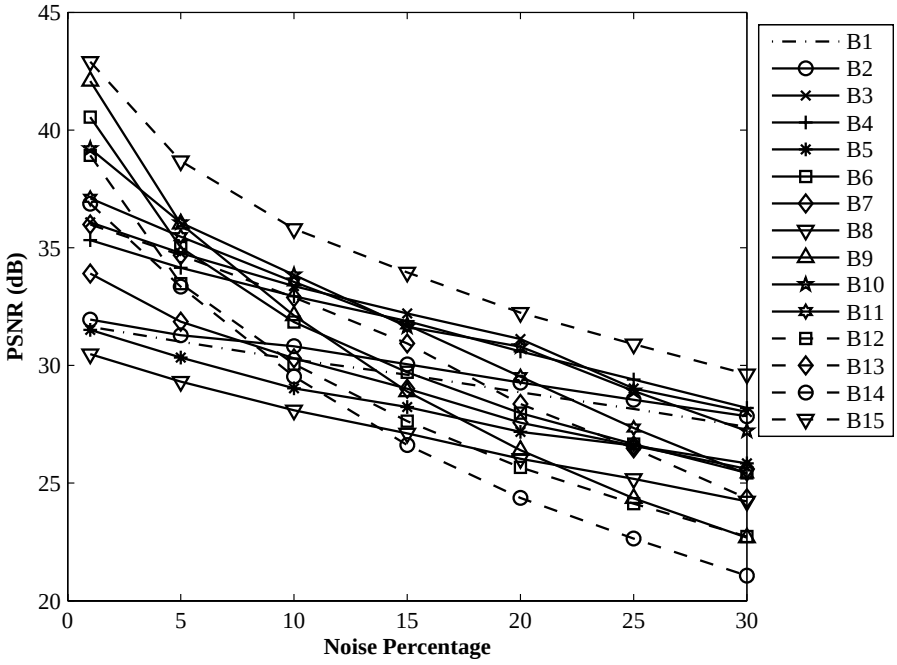

Figure 1.6: PSNR (dB) variations of *Lena* image corrupted with RVIN by Group-B schemes

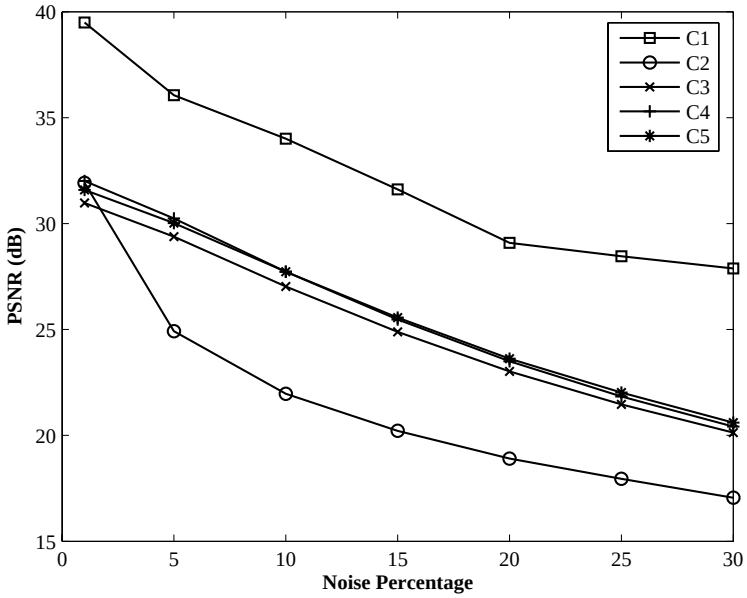

Figure 1.7: PSNR (dB) variations of *Lena* image corrupted with RVIN by Group-C schemes

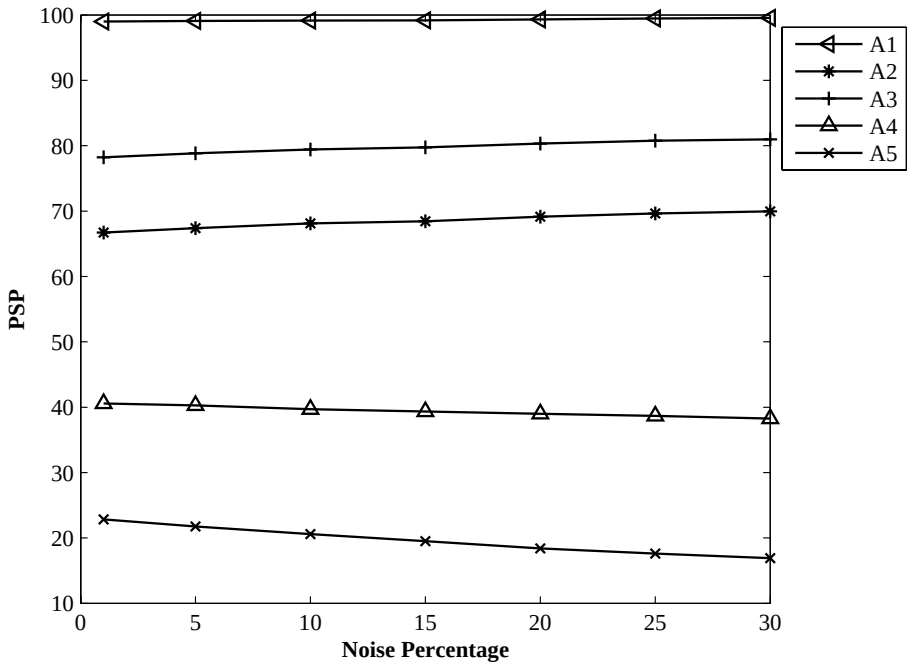

Figure 1.8: PSP variations of *Lena* image corrupted with RVIN by Group-A schemes

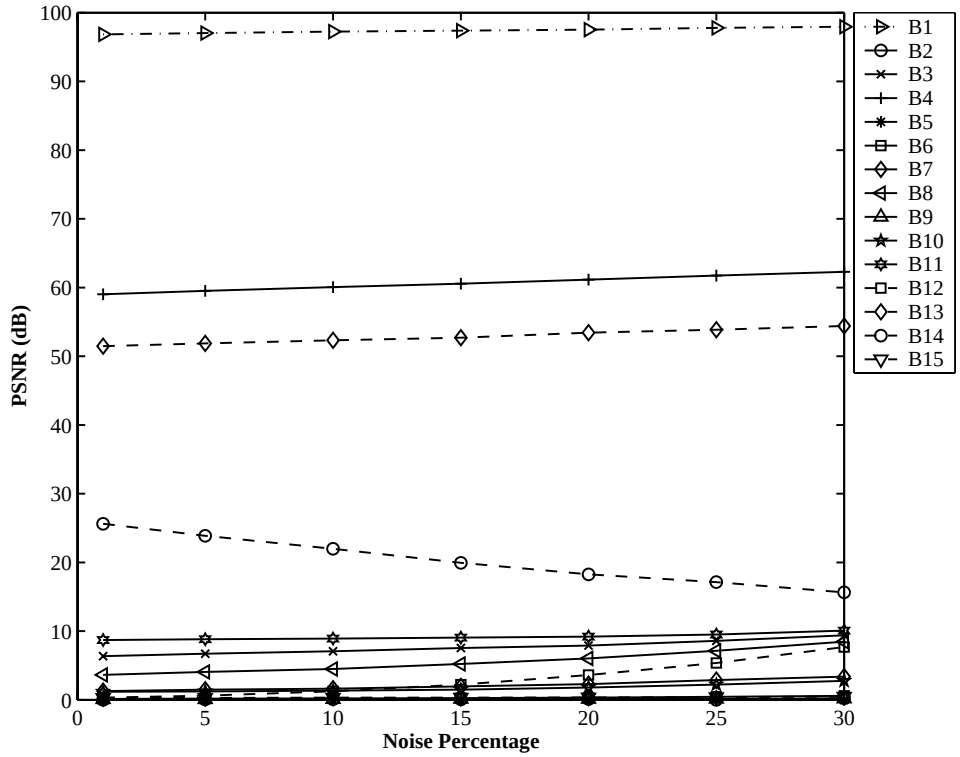

Figure 1.9: PSP variations of *Lena* image corrupted with RVIN by Group-B schemes

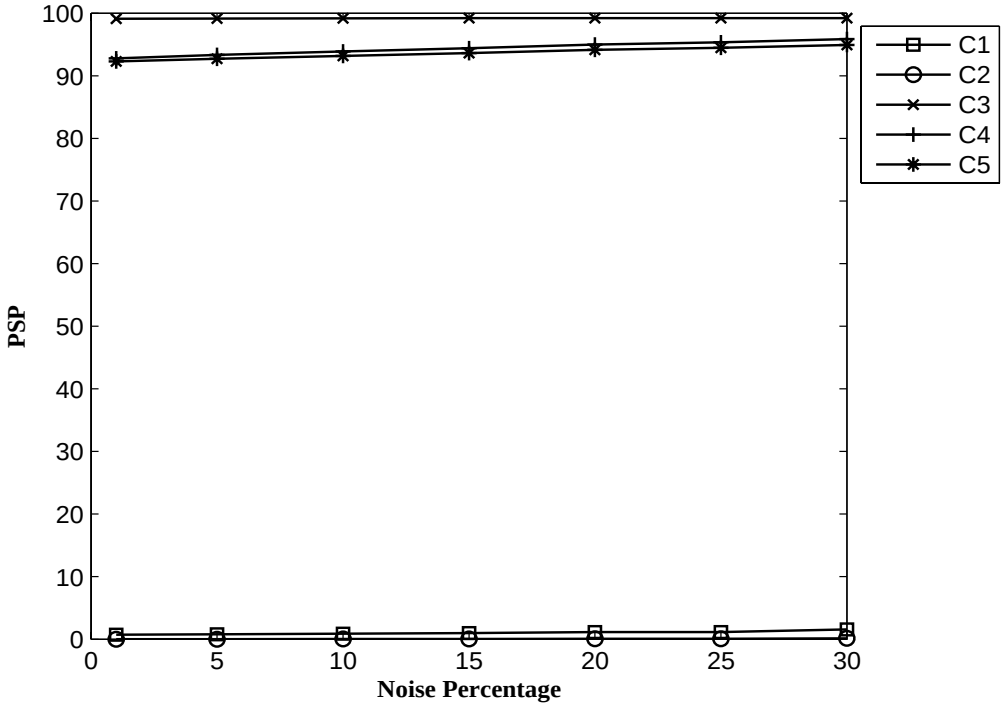

Figure 1.10: PSP variations of *Lena* image corrupted with RVIN by Group-C schemes

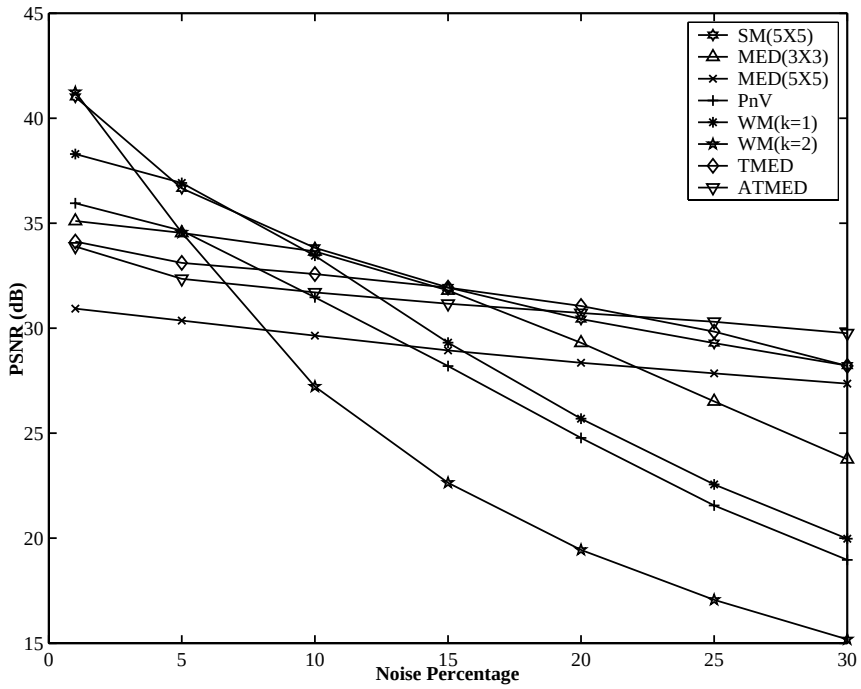

Figure 1.11: PSNR (dB) variations of *Lena* image corrupted with SPN

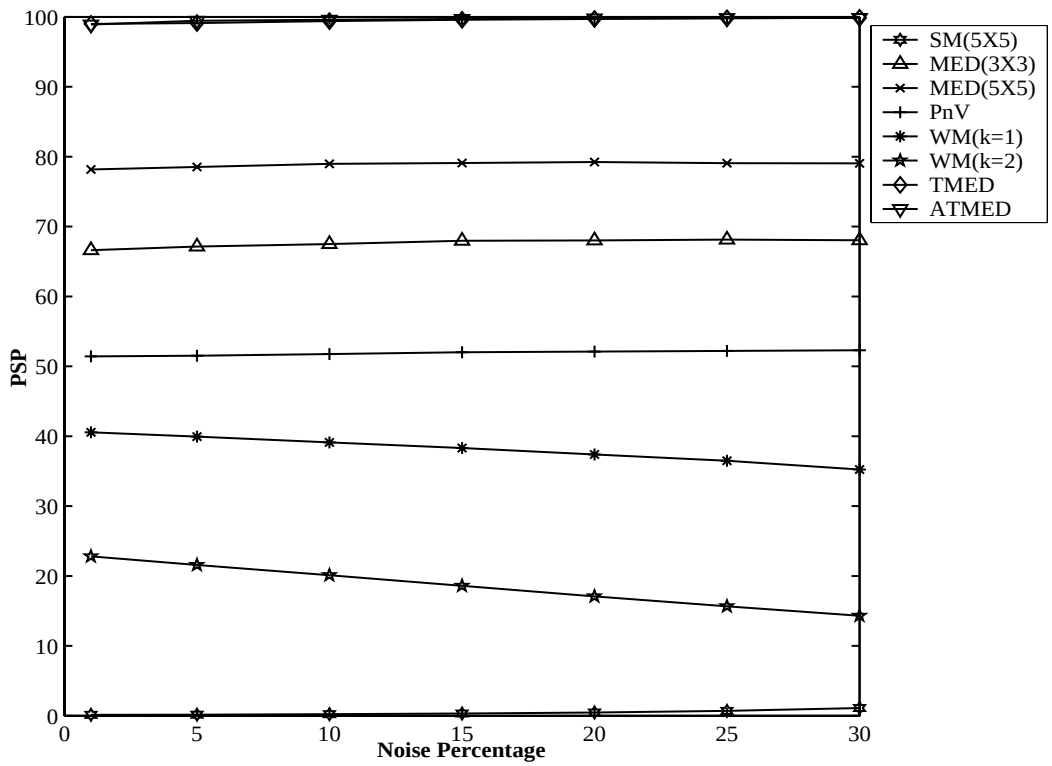

Figure 1.12: PSP variations of *Lena* image corrupted with SPN

(a) $\alpha 1$ (b) $\alpha 2$ (c) $\alpha 3$

(d) $\beta 1$ (e) $\beta 2$ (f) $\beta 3$

Figure 1.13: Subjective Evaluation of *Lena* image subjected to Cascaded Noise Reduction and Sharpness Enhancement schemes

Chapter 2

Adaptive Threshold for Impulsive Noise Detection

The pending problem that research in *Random Valued Impulsive Noise* (RVIN) filtering has been facing is the inability to distinguish noisy values that do not occur as extreme outliers in comparison with surrounding pixels. *Salt and Pepper* (SPN) handling is easy whereas RVIN noise cases are difficult to deal with and most research directions triala are towards removal of RVIN noise from images. we have observed few contribution in this directions which has been discussed in this chapter and the following chapter. The proposed detection scheme involves second order difference of pixels, which is described in Section 2.1. Threshold values are selected for impulse detection using different image statistics and neural models. The need for adaptive threshold is described in Section 2.2. *Multilayer Perceptron based Adaptive Thresholding* (MLPAT) for impulse detection is discussed in Section 2.3. In Section 2.4, a Functional Link Artificial neural Network is used to determine the adaptive threshold named, *Image Statistics based Adaptive Thresholding* (ISAT) is presented. *Radial Basis Functional Network based adaptive thresholding* (RBFNAT) for impulse detection is the second noise detection scheme presented in Section 2.5. Section 2.6 presents a comparative analysis of the proposed schemes with some of the well accepted schemes. Finally, Section 2.7 provides a complete summary of the chapter.

2.1 Second Order Difference of Pixels

First and second order derivative must be considered in a digital context before using it for impulse detection. The behavior of these derivatives in the areas of constant gray level, at the onset and end of discontinuities, and along gray level ramps of an image is required to be studied. On the basis of this study we can say the discontinuities in an image can be used to model noise points, lines and edges. The behavior of derivatives during transitions into and out of these image features also is of interest. So for the sake of simplified explanation, one-dimensional derivative is focused initially in a digital context. The derivatives of a digital function are defined in terms of differences. Any definition we use for first derivative that must be:

i. zero in the areas of constant gray level values i.e. flat segment,

ii. nonzero at the onset of a gray level step or ramp and along the ramp.

Similarly in that context, the second difference must be:

i. zero in the flat areas and along ramps of constant slopes,

ii. nonzero at the onset and end of a gray level step or ramp.

Since derivatives are found for digital quantities whose values are finite, the maximum possible gray level change is also is finite, and the shortest distance over which that change can occur is between adjacent pixels. First-order derivative of a one-dimensional function $f(x)$ may be defined as:

$$\frac{\partial f}{\partial x} = f(x+1) - f(x) \tag{2.1}$$

Similarly, second-order derivative may be defined as:

$$\frac{\partial^2 f}{\partial x^2} = f(x+1) + f(x-1) - 2f(x) \tag{2.2}$$

Figure 2.1 shows a horizontal gray level profile of the edge between two regions. Also the first and second difference of the gray level profile are shown in the figure. From left to right along the profile, the first difference is positive at the points of

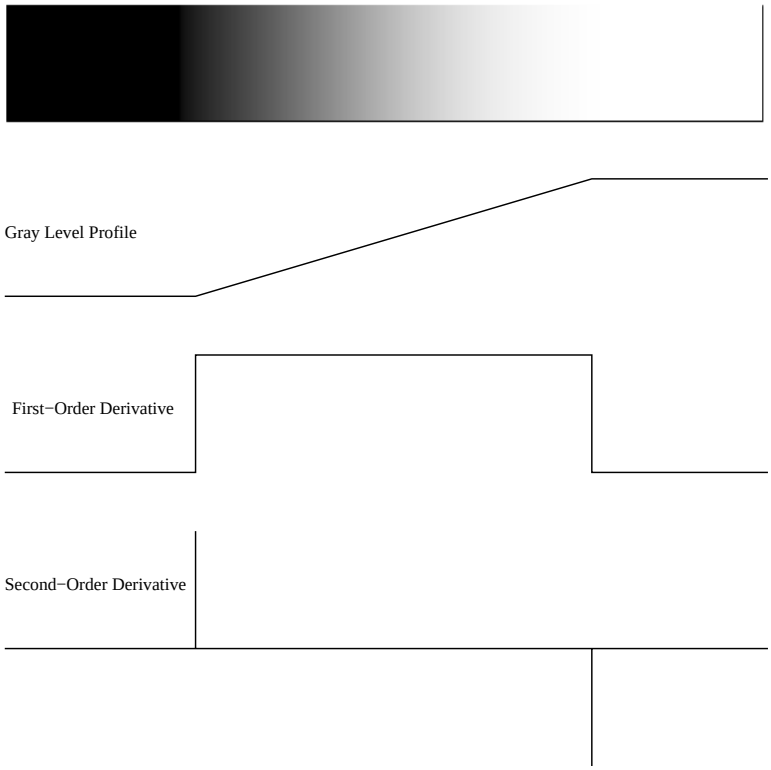

Figure 2.1: Gray level profile, first-order and second-order derivative of an image

transition into and out of the ramp; and is zero in the flat segment. The second derivative is zero except at the transition points [3].

This behavior of second difference is exploited in the proposed schemes to determine the sanctity of a pixel. An impulse is nothing but the change in gray level profile of an image. The second difference of an impulse will result in a spike. Also there will be a spike for an edge. In order to differentiate between these two spikes a second order difference based impulse detection mechanism is employed at location of the test pixel. Once a test pixel is identified as an impulse it is immediately filtered by replacing it with the median of the surrounding pixels. This filtered pixel also takes part in the noise detection phase of the next test pixel and subsequent filtering, if needed. The detection (and filtration)is done twice, once in the horizontal direction and again in the vertical direction, thus each test pixel is compared with its neighbors in both directions. Hence selective filtering helps in achieving superb visual quality and remove the noise completely at all noise conditions.

The noise detection algorithm is applied in both horizontal and vertical passes as described in Section 2.1.1 in detail.

Selection of noise threshold is an important task in the noise detection algorithm and is described in Section 2.2. It should be noticed that the threshold used in both the directions are different and is obtained using a neural detector.

2.1.1 Algorithm

The proposed algorithm consists of two passes and is described below:

Pass One

i. Choose a window $X^{(t)}$ of size 3×5 located at the top-left corner of the observed image X.

$$X^{(t)} = \begin{pmatrix} X_{i-1,j-2} & X_{i-1,j-1} & X_{i-1,j} & X_{i-1,j+1} & X_{i-1,j+2} \\ X_{i,j-2} & X_{i,j-1} & X_{i,j} & X_{i,j+1} & X_{i,j+2} \\ X_{i+1,j-2} & X_{i+1,j-1} & X_{i+1,j} & X_{i+1,j+1} & X_{i+1,j+2} \end{pmatrix} \tag{2.3}$$

Consider a 3×3 sub-window $X^{(w)}$ from X as:

$$X^{(w)} = \begin{pmatrix} X_{i-1,j-1} & X_{i-1,j} & X_{i-1,j+1} \\ X_{i,j-1} & X_{i,j} & X_{i,j+1} \\ X_{i+1,j-1} & X_{i+1,j} & X_{i+1,j+1} \end{pmatrix} \tag{2.4}$$

ii. Compute the first order 3×4 difference matrix $f^{(d)}$ from $X^{(t)}$ as:

$$f^{(d)} = \begin{pmatrix} f^{(d)}_{i-1,j-1} & f^{(d)}_{i-1,j} & f^{(d)}_{i-1,j+1} & f^{(d)}_{i-1,j+2} \\ f^{(d)}_{i,j-1} & f^{(d)}_{i,j} & f^{(d)}_{i,j+1} & f^{(d)}_{i,j+2} \\ f^{(d)}_{i+1,j-1} & f^{(d)}_{i+1,j} & f^{(d)}_{i+1,j+1} & f^{(d)}_{i+1,j+2} \end{pmatrix} \tag{2.5}$$

where $f^{(d)}_{i+k,j+l} = X^{(t)}_{i+k,j+l} - X^{(t)}_{i+k,j+l-1}$, $k = -1, 0, 1$ and $l = -1, 0, 1, 2$.

iii. Compute the second order 3×3 difference matrix $s^{(d)}$ from $f^{(d)}$ as:

$$s^{(d)} = \begin{pmatrix} s^{(d)}_{i-1,j-1} & s^{(d)}_{i-1,j} & s^{(d)}_{i-1,j+1} \\ s^{(d)}_{i,j-1} & s^{(d)}_{i,j} & s^{(d)}_{i,j+1} \\ s^{(d)}_{i+1,j-1} & s^{(d)}_{i+1,j} & s^{(d)}_{i+1,j+1} \end{pmatrix} \tag{2.6}$$

where $s^{(d)}_{i+p,j+q} = f^{(d)}_{i+p,j+q+1} - f^{(d)}_{i+p,j+q}$, $p = -1, 0, 1$ and $q = -1, 0, 1$.

iv. The decision index $d_{i,j}$ at (i, j) is then computed as:

$$d_{i,j} = \begin{cases} 0 & \text{if } \left|s^{(d)}_{i,j}\right| > \theta_1 \\ 1 & \text{otherwise} \end{cases} \tag{2.7}$$

Select threshold θ_1 as described in Sections 2.2– 2.5.

v. Use median filter on the noisy pixels only to remove noise from the pixel (i, j) with the sub-window as in (2.4).

vi. Shift the window $X^{(t)}$ one by one column from left to right and top to bottom (as shown in Figure 2.2(a)) and for all windows repeat the steps (ii) through (vi).

Pass Two

i. Repeat steps (i) through (vi) of Pass One (as shown in Figure 2.2(b)) with $X^{(t)}$ order as 5×3, $f^{(d)}$ order as 4×3, and the threshold value as θ_2 in place of θ_1.

2.2 Adaptive Threshold Selection

The sanctity of a pixel is decided solely by the threshold. If a predefined parameter of a test pixel exceeds the threshold value, it is termed as contaminated. Solution to image restoration problem depends very much on the type of image, characteristics and density of noise. It is observed from the following experiment that a single threshold value does not serve the purpose as well as in different noise conditions. The steps are described as follows:

i. An image (say *Lena*) is corrupted with impulsive noise of densities 1%, 5%, 10%, 15%, 20%, 25%, and 30%.

ii. The first noisy image $Lena_1$ (the subscript is for 1% of noise) is subjected to the proposed algorithm outlined in Section 2.1.1 by varying the threshold value θ between 0 and 1.

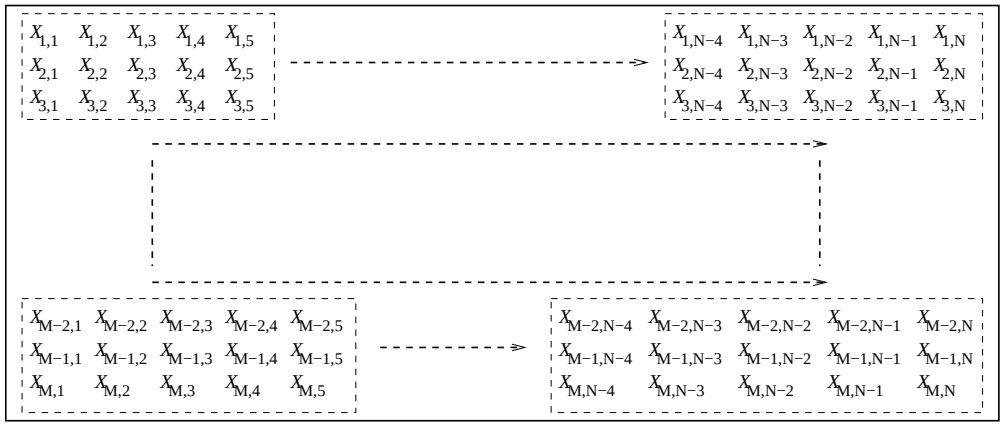

(a) Horizontal Direction

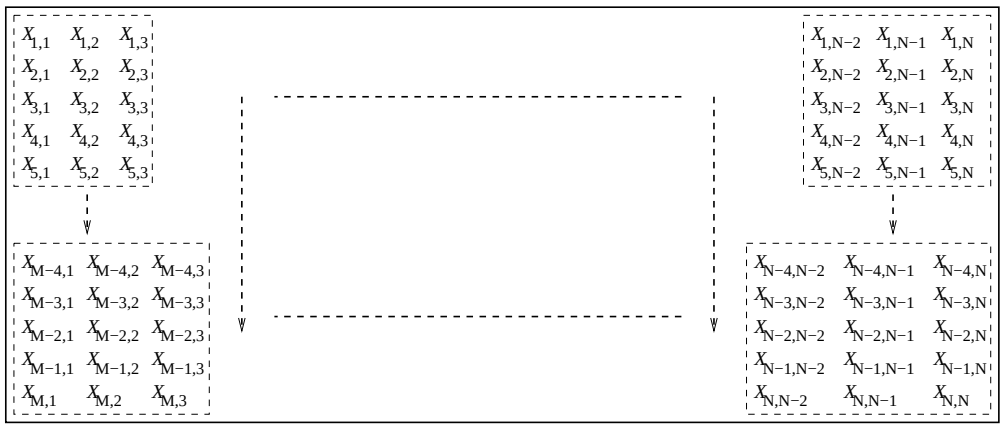

(b) Vertical Direction

Figure 2.2: Window Selection for an $M \times N$ Image

iii. The MSE(dB) for each threshold is computed and plotted as shown in Figure 2.3. The plot shows that the image achieves minimum MSE for 1% noise, denoted as $\text{MSE}_{min}^{(1)}$ at $\theta = 0.29$ and let this threshold be denoted as $\theta_{opt}^{(1)}$.

iv. Similarly, $\theta_{opt}^{(i)}$ are obtained by recording the minimum MSE $\text{MSE}_{min}^{(i)}$ for $i \in \{5, 10, 15, 20, 25, 30\}$ percentage of noise densities.

v. The relationship between optimum threshold versus the noise densities is shown in Figure **??**. This clearly reveals that threshold needs to be different at different at different noise densities to minimise the error and hence to maximise the PSNR (dB) in restored images.

vi. The overall relationshipsbetween MSE(dB) and its corresponding optimum threshold for different noise conditions for *Lena* image is shown in Figure 2.4.

vi. Similar steps are repeated for other standard images like *Lisa*, *House*, *Peppers* etc. The observations are plotted in Figures 2.5(a), 2.5(b), 2.5(c) and 2.5(d).

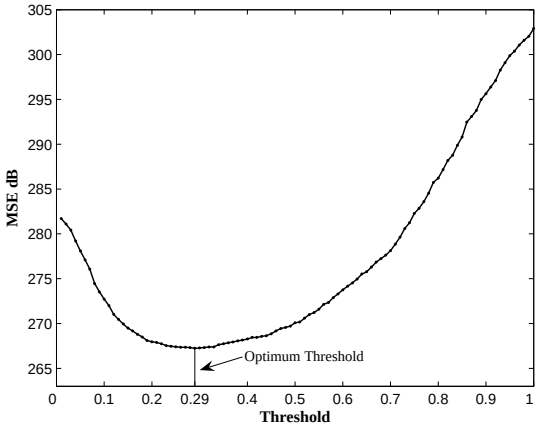

Figure 2.3: Variation of MSE for different threshold values for 1% RVIN noise for *Lena* image.

It is in general observed that, there exists an optimum threshold for every image and for a particular noise density. Even these values differ from image to image for the same noise density. In addition, the plots reveals clearly that there exists nonlinear relationship between optimum threshold and noise densities as well as MSE.

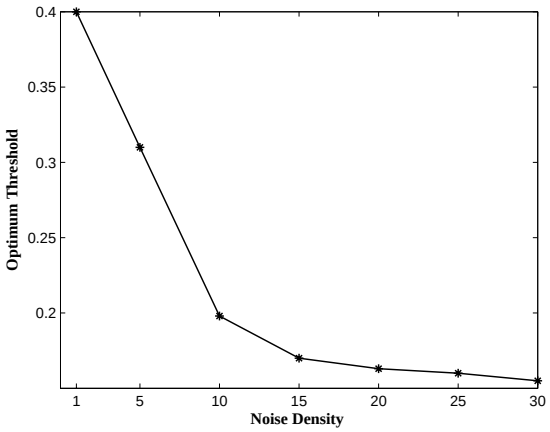

Figure 2.4: Variation of Optimum threshold for different noise % for *Lena* image.

The experimental results gives a direction that if an optimum threshold can be derived adaptively from a given noisy image, the noise detection becomes efficient

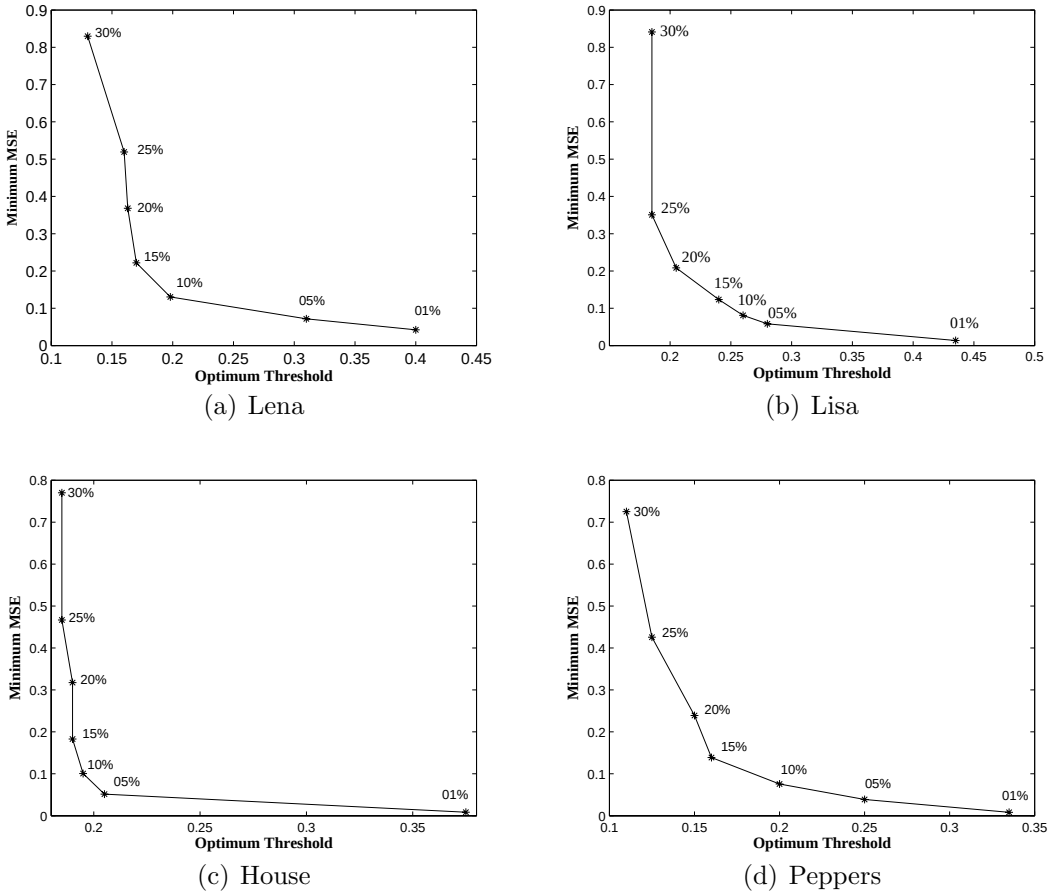

(a) Lena (b) Lisa

(c) House (d) Peppers

Figure 2.5: Variation of Minimum MSE at different Threshold values

and in turn will affect the filtering performance. But to predict the threshold, neither the parameters like the noise percentage nor MSE will be a help in real time image processing as both need the knowledge of original image which is not available. Hence, a parameter which can be derived from the given noisy image will be of great help to handle real life situations. For the purpose, a statistical parameter called *Coefficient of Variance* (CV) for a noisy image is defined as:

$$\mathrm{CV} = \frac{\sigma}{\mu} \tag{2.8}$$

where, σ and μ are the standard deviation and mean of the noisy image respectively. To further extend the experiment we compute the CVs for all noisy images for *Lena* i.e $\mathrm{CV}^{(i)}$, for $i \in \{5, 10, 15, 20, 25, 30\}$. The relation between CVs and the optimum threshold is shown in Figure 2.6. This figure also gives the additional information regarding the existence of a non linear relationship between these two parameters. Hence, it is decided to utilise the computable parameters, μ, σ^2, CV from a noisy image to predict optimum threshold. Neural network being the candidate for a non linear predictor, various neural architectures have been exploited for the purpose.

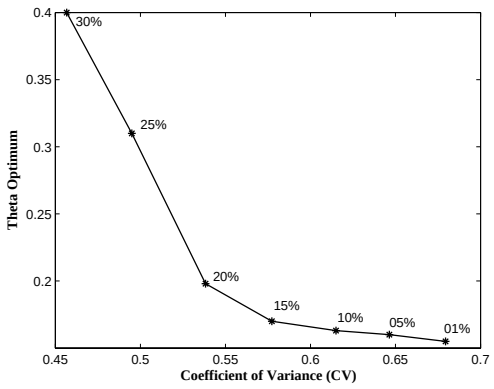

Figure 2.6: Variation of Optimum threshold with CV at different noise density for *Lena* image.

2.3 Adaptive Thresholding for Impulse Detection using MLP

Over the past few years, a view has emerged that computing based on the structure and function of the biological neural networks may hold the key to the success

of solving intelligent tasks. The new field is called *Artificial Neural Networks* (ANN), although it is more appropriate to describe it as parallel and distributed processing [59]. An ANN consists of interconnected processing units and has a natural tendency to store knowledge for further use. ANN serves as a potential tool for numerous nonlinear problems. The ANN based signal detection and filtering schemes are robust, accurate and work well under nonlinear situations [4].

An ANN consists of interconnected processing units. Typically each processing unit consists of a summing part followed by an output part. Each summing part receives a number of input values from a group of other neurons or from external stimulus. It weights each value, and computes a weighted sum. This weighted sum is called activation value and constitutes the arguments to a nonlinear activation function. The resulting value of the activation function is the output of the neuron. This output gets distributed along weighted connections to other neurons. The actual manner in which these connections are made defines the flow of information in the network and called architecture of the ANN.

A neural network has to be configured such that the application of a set of inputs produces the desired set of outputs. This is achieved by updating the weights and the process of training the network are called learning paradigms. The learning paradigms may be supervised, unsupervised or reinforced [11]. Typically neural networks consists of at least two layers of neurons—a hidden layer and an output layer. The hidden layer neurons should have nonlinear and differentiable activation functions. The nonlinear activation functions enable a neural network to be a universal approximator. The problem of representation is solved by the nonlinear activation functions [60].

Multilayer perceptron (MLP) networks is an important class of neural networks. MLP network consists of a set of simple sensory units called perceptrons. These sensory unit constitute the input layer and one or more hidden layer of the network. The input signal passes through the network in the forward direction making it a feed forward neural network. MLP is the most widely used neural classifier for which many learning paradigms have been developed and it belongs to

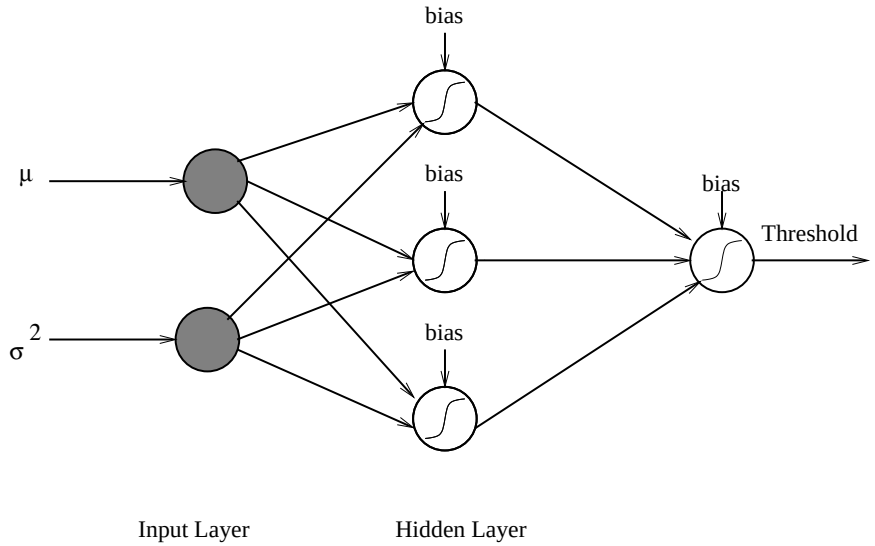

Figure 2.7: Multi-Layer Perceptron Structure of Threshold (θ_1) Estimator.

the class of supervised neural networks [11]. In MLP networks there exists a non-linear activation function. The hidden layers along with the connected synaptic weights make the MLP network active for highly complex tasks.

Here in this section a simple 2–3–1 multi layer perceptron (MLP) (Figure 2.7) is used to adapt the image environment and to provide an optimal threshold value for impulsive noise detection. Both the noisy image characteristics (Section 2.2) mean (μ) and variance (σ^2) of *Lisa*, *House*, *Gatlin* and *Peppers* images are obtained. These two statistical parameters along with corresponding θ_{opt} of these four images are used here to prepare the training dataset. The suggested neural network is trained with the available training dataset using the conventional back propagation algorithm [61]. The Back propagation Algorithm trains the MLP for a given set of input patterns with known classifications. μ and σ^2 of the noisy image are used as the two inputs parameters to the perceptron network and θ_{opt} is used as the target output of the network. The training convergence characteristics of the network is obtained and is shown in Figure 2.8.

The neural network with trained weights are used to obtained threshold subsequently. It is observed that the neural network can predict accurate threshold for images that are not at all used for training.

First pass of the noise detection algorithm(2.1.1) uses the threshold value

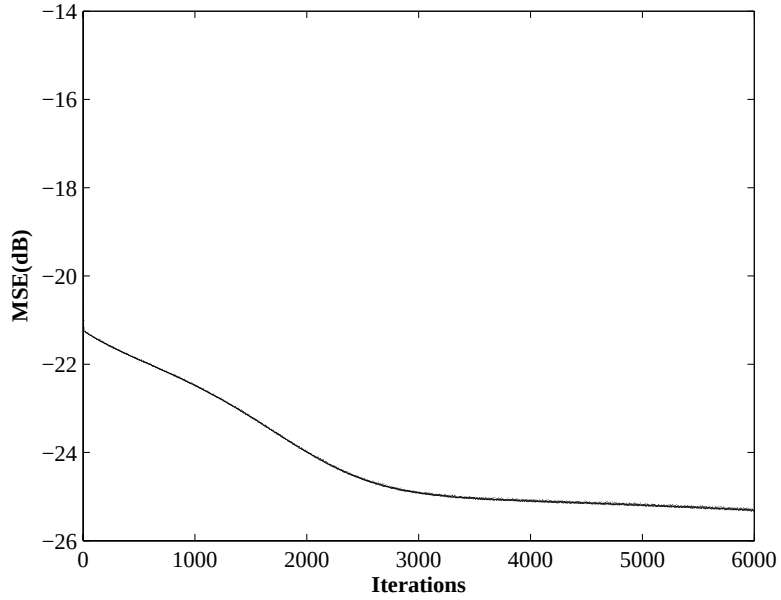

Figure 2.8: Convergence Characteristics of Multilayer Perceptron Network

obtained using the MLP. The output image of the first pass is then subjected to second pass of the algorithm. In the second pass a different θ is used. Mean and variance of the output image of the first pass is fed to the network to get the new threshold value to be used in the second pass.

2.4 Image Statistics based Adaptive Thresholding using FLANN

The Functional Link Artificial Neural Network (FLANN) has been developed as an alternative architecture to the well–known Multi-Layer Perceptron (MLP) net with application to both function approximation and pattern recognition [62]. The main advantage of using FLANN is reduced computational cost in the training stage, while maintaining the approximation performance of the MLP network. It is basically a flat net and the need of the hidden layer is removed. The functional expansion effectively increases the dimensionality of the input vector and hence the hyperplanes generated by the FLANN provides greater discrimination capability in the input pattern space [62, 63].

A Functional Link Artificial Neural Network has a feedforward architecture with a number of non-linear enhancement hidden nodes, referred to as functional

links. This proposed detector (FLANN) is shown in Figure 2.9. It is a two layers structure. The parameters used in the training are same as that of previous section and are derived from the input noisy image. Mean and variance are the two statistical inputs which are functionally expanded in the input layer with the trigonometric polynomial basis functions given by:

$$\{1, \mu, sin(\pi\mu), \cdots, sin(N\pi\mu), cos(\pi\mu), \cdots, cos(N\pi\mu),$$

$$\sigma^2, sin(\pi\sigma^2), \cdots, sin(N\pi\sigma^2), cos(\pi\sigma^2), \cdots, cos(N\pi\sigma^2)\}$$

In order to calculate the error, the actual output on the output layer is compared with the desired output. Depending on this error value, the weight matrix between the input–output layers is updated using back propagation learning algorithm. The training convergence characteristics of the network is shown in Fig. 2.10.

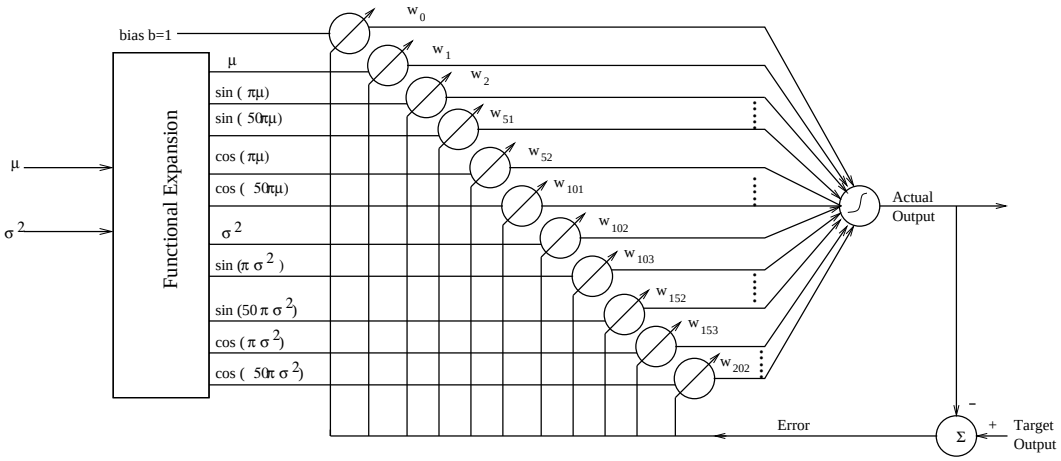

Figure 2.9: Functional Link Artificial Neural Network (FLANN) Structure for Threshold Estimation

This threshold value is used in the first pass of the algorithm to detect impulses in the horizontal direction. The filtered image obtained after the first pass is then subjected to second pass of the algorithm, where impulses are detected in vertical fashion. In the second pass a different θ is used. Using the mean and variance of the output image of the first pass new threshold value for the second pass is computed.

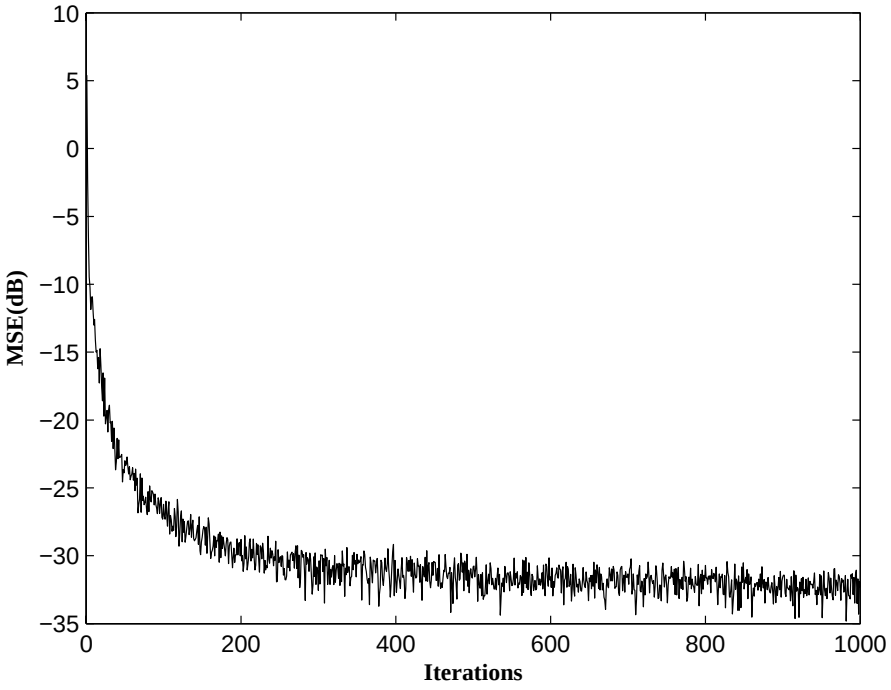

Figure 2.10: Convergence Characteristics of FLANN structure

2.5 RBFN based Adaptive Threshold Selection for Detecting Impulsive Noise in Images

Radial Basis Functional Network (RBFN) have gained considerable attention as an alternate to multilayer perceptrons trained by the back propagation algorithm. The basis function are embedded in a two layer neural network, where each hidden unit implements a radial activated function. There are no weights connected between the input layer and hidden layer. The output units implement a weighted sum of hidden unit outputs. The input into an RBF network is nonlinear while the output is linear. The RBF's are characterized by there localization (center) and by an activation hyperspace(activation function). The activation function used in a RBFN is usually a localized Gaussian basis function. In this detection scheme we use the standard Gaussian nonlinearity basis function as defined in (2.9).

$$\phi_{\mathrm{i}}(x) = exp(-\frac{(x - c_i)^2}{2\sigma^2}) \tag{2.9}$$

Each gaussian basis function consists of a center (c_i) and a variance σ^2 as its input parameters. The spread σ of all the Gaussian basis function has been taken fixed

and a standard value of 0.1 is used. Basis function centers can be randomly sampled among the input instances or obtained by Orthogonal Least Square Learning Algorithm or found by clustering the samples and choosing the cluster means as the centers. Since our training data set is limited so the centers are randomly selected from the training sample and are used to compute ϕ_i. The distance metric employed to calculate the distance of the inputs from the basis center is Euclidean distance.

The proposed neural detector is a two layers structure and is shown in Figure 2.11. Finding the appropriate RBF weights is called network training and

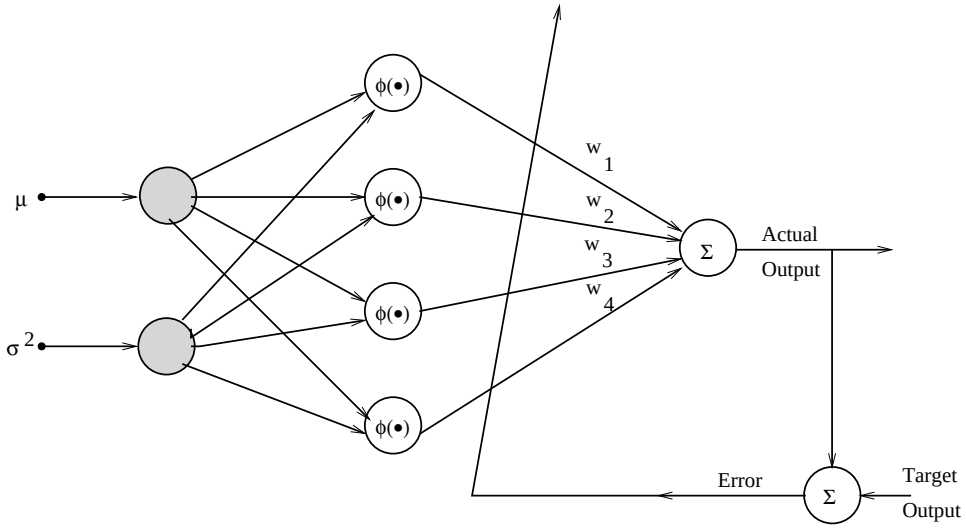

Figure 2.11: Radial Basis Functional Network (RBFN) Structure for Threshold Estimation

Least Mean Square(LMS) learning algorithm is applied. The parameters used for training are same as that of previous section (2.3). Mean and variance of the noisy image are the two input parameters to the input layer of the network used to obtain the noise threshold. Using a set of input–output pair (training data set) we optimize the network parameters using LMS. In order to determine the error, the actual output on the output layer is compared with the desired output. Depending on this error value, the weight matrix between the input–output layers is updated. The training convergence characteristics of the network is shown in Figure 2.12.

The threshold value obtained using RBFN is used in the first pass of the algo-

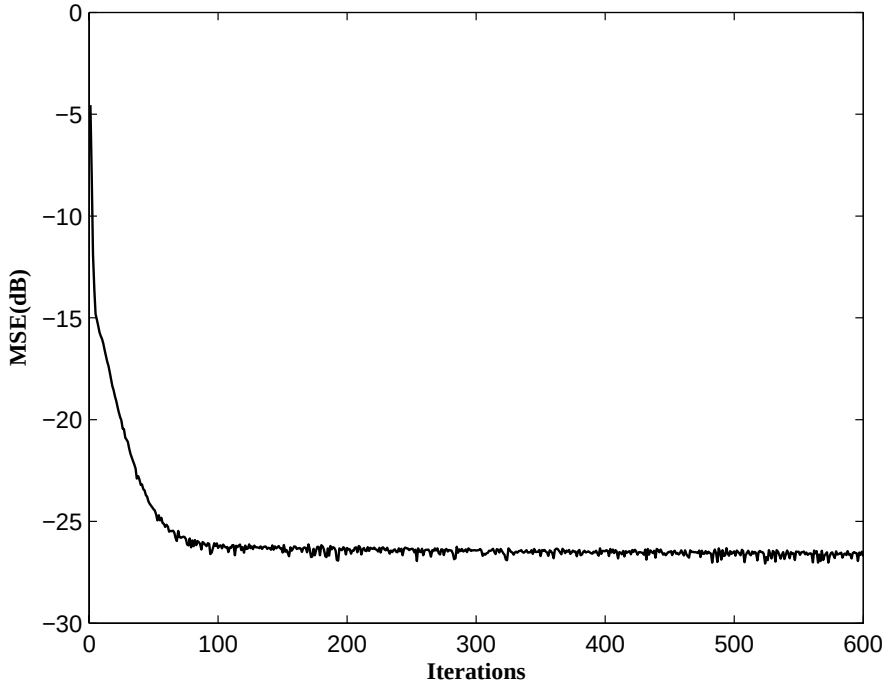

Figure 2.12: Convergence Characteristics of Radial Basis Functional Network

rithm to detect impulses in the horizontal direction. The filtered image obtained after the first pass is then subjected to second pass of the algorithm, where impulses are detected in vertical fashion. In the second pass a different threshold is used. Using the mean and variance of the output image of the first pass new threshold value for the second pass is computed. All the steps of first iteration is repeated in the second iteration with the new threshold.

2.6 Simulations and Results

The three proposed schemes (MLPAT, ISAT, RBFNAT) are simulated with some of the best performing schemes reviewed in Section 1.6. Adaptive Two-Pass Median filter (2-Pass) [57], Adaptive Center Weighted Median Filter (ACWMF) [29], Signal Dependent-Rank Ordered Mean (SD-ROM) [41], Tri-State Median (TSM) [42], Pixel Wise MAD (PWMAD) [37] and Second Order Differential Impulse Detector (SODID) [64] are used for comparison. *Lena* image is corrupted with *Random Valued Impulsive Noise* of 1% to 30% noise densities. These noisy images are subjected to filtering by the proposed schemes (MLPAT, ISAT, RBFNAT) along

with the above six existing schemes. The PSNR (in dB) and PSP (in percentage) thus obtained are plotted in Figures 2.13 and 2.14 respectively.

Similarly, simulations are conducted with other standard images like *Lisa*,*Girl*, *Clown*, *Gatlin*, *Bridge*, *Boat* and *Peppers*. Table 2.1 lists the PSNR obtained at 15% and 20% of RVIN. Another listing is shown in Table 2.2 for PSP at the same noise densities.

Two subjective comparisons are also made in Figures 2.15 and 2.16. The former figure shows the restored images of *Lena* corrupted with 15% of noise density and the later one shows restored images of *Peppers* corrupted with 20% noise density.

The performance of the proposed schemes in terms of $PSNR(dB)$ are better than most of the schemes except SDROM and TSM. However, both the proposed schemes are computationally better than the above two techniques (listed in Table 2.3). This is verified by simulating the schemes in Matlab 7.0, Microsoft Windows XP (SP2) Operating System and Intel Pentium D–2.80 GHz with 1GB of RAM.

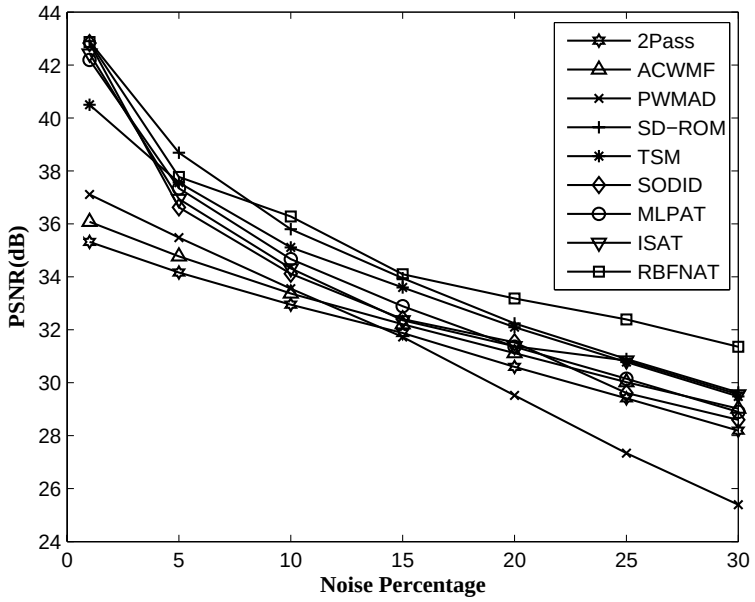

Figure 2.13: PSNR (dB) variations of Restored *Lena* image corrupted with RVIN of varying strengths by different adaptive threshold schemes

Table 2.1: PSNR (dB) of different adaptive schemes at 15% and 20% of noise on different images

		Lisa	*Girl*	*Clown*	*Gatlin*	*Bridge*	*Boat*	*Peppers*
	2Pass	31.34	29.62	22.84	31.59	25.77	29.33	31.55
	ACWMF	31.78	30.04	22.56	31.62	25.36	28.87	32.98
	PWMAD	30.50	29.28	23.02	30.66	26.07	29.25	31.29
15%	SD-ROM	31.98	31.31	24.33	32.77	27.48	30.75	32.00
RVIN	TSM	32.05	31.05	23.88	32.46	27.08	30.51	33.04
	SODID	30.71	30.19	24.52	31.71	26.76	29.59	31.87
	MLPAT	29.86	30.20	22.97	31.67	26.68	29.98	32.04
	ISAT	31.79	30.17	23.59	31.83	17.42	28.93	32.15
	RBFNAT	32.46	29.39	26.20	32.77	26.13	29.67	34.34
	2Pass	30.46	28.41	22.25	30.45	25.09	28.32	30.14
	ACWMF	30.97	29.92	23.56	31.34	24.82	28.10	31.50
	PWMAD	28.26	27.73	22.16	28.77	24.99	27.57	29.04
20%	SD-ROM	30.86	29.92	23.59	31.51	26.55	29.50	31.40
RVIN	TSM	30.95	29.69	23.28	31.30	26.28	29.35	31.41
	SODID	28.89	28.66	22.82	30.14	25.82	28.41	30.24
	MLPAT	29.90	29.11	22.38	30.67	25.83	28.81	30.55
	ISAT	30.37	28.14	21.69	29.49	16.64	28.18	30.48
	RBFNAT	31.73	28.47	26.16	31.34	25.55	28.88	33.16

2.7 Summary

This chapter proposes an improved filtering scheme for suppressing impulsive noise of varying strengths from corrupted images. The threshold value used for detection of impulsive noise is suggested to be an adaptive one. This leads to reliable detection of corrupted pixels. The filtration is thus performed selectively only on the detected noisy pixels. Hence undue distortion is eliminated in the restored images. In this chapter two different ways of determining the threshold values are presented. Along with MLP, various neural architecture i.e FLANN, RBFN was used to determine the threshold. The proposed scheme's performances are poor for some images when compared with existing schemes. However, computationally the proposed schemes are well off.

Table 2.2: PSP of different adaptive schemes at 15% and 20% of noise on different images

		Lisa	*Girl*	*Clown*	*Gatlin*	*Bridge*	*Boat*	*Peppers*
	2Pass	35.23	51.76	51.95	31.75	54.73	67.30	67.41
	ACWMF	6.93	13.29	38.68	5.57	27.98	15.27	0.55
	PWMAD	7.35	11.05	24.85	4.00	15.83	13.95	10.53
15%	SD-ROM	0.14	0.93	10.29	0.39	3.06	1.04	0.34
RVIN	TSM	0.22	2.62	17.51	0.98	7.94	2.55	0.57
	SODID	4.84	11.56	19.94	8.34	15.54	13.00	12.16
	MLPAT	4.65	11.16	36.87	8.11	15.36	11.16	10.55
	ISAT	11.82	62.63	54.04	13.11	0.01	73.98	23.65
	RBFNAT	3.69	6.29	13.88	11.68	27.80	28.87	17.54
	2Pass	35.67	58.10	52.98	33.24	55.71	67.50	67.45
	ACWMF	0.60	0.43	12.60	0.41	28.69	15.80	0.57
	PWMAD	7.06	7.82	22.78	5.03	15.10	13.18	10.05
20%	SD-ROM	0.18	0.40	9.86	0.33	3.10	1.11	0.37
RVIN	TSM	0.31	1.21	21.07	1.00	8.30	2.82	0.73
	SODID	6.52	16.74	24.37	10.10	18.75	16.85	15.92
	MLPAT	6.25	17.84	42.46	10.10	18.50	14.70	14.11
	ISAT	40.17	65.59	56.85	12.38	0.06	74.21	55.98
	RBFNAT	11.82	62.63	54.04	13.11	0.01	73.98	23.65

Table 2.3: Computational time for different Schemes for removing impulsive noise from *Lena* image corrupted with 15% of RVIN

Scheme	Time (sec)
2-PASS	149.19
ACWMF	413.03
PWMAD	234.68
SDROM	11.60
TSM	74.34
SODID	10.72
MLPAT	11.97
ISAT	11.16
RBFNAT	4.09

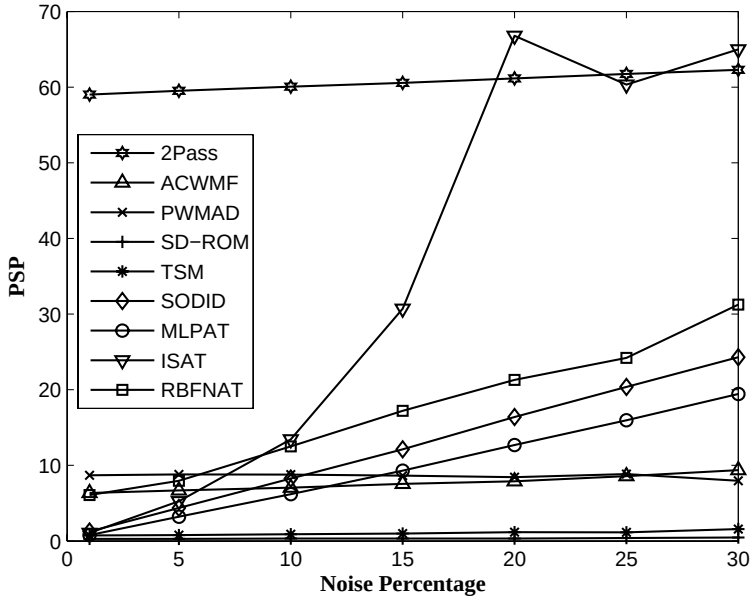

Figure 2.14: PSP variations of Restored *Lena* image corrupted with RVIN of varying strengths by different adaptive threshold schemes

(a) True Image (b) 15% Noisy

(c) 2-Pass (d) ACWMF (e) PWMAD

(f) SDROM (g) TSM (h) SODID

(i) MLPAT (j) ISAT (k) RBFNAT

Figure 2.15: Impulsive Noise filtering of *Lena* image corrupted with 15% of RVIN by different adaptive threshold schemes

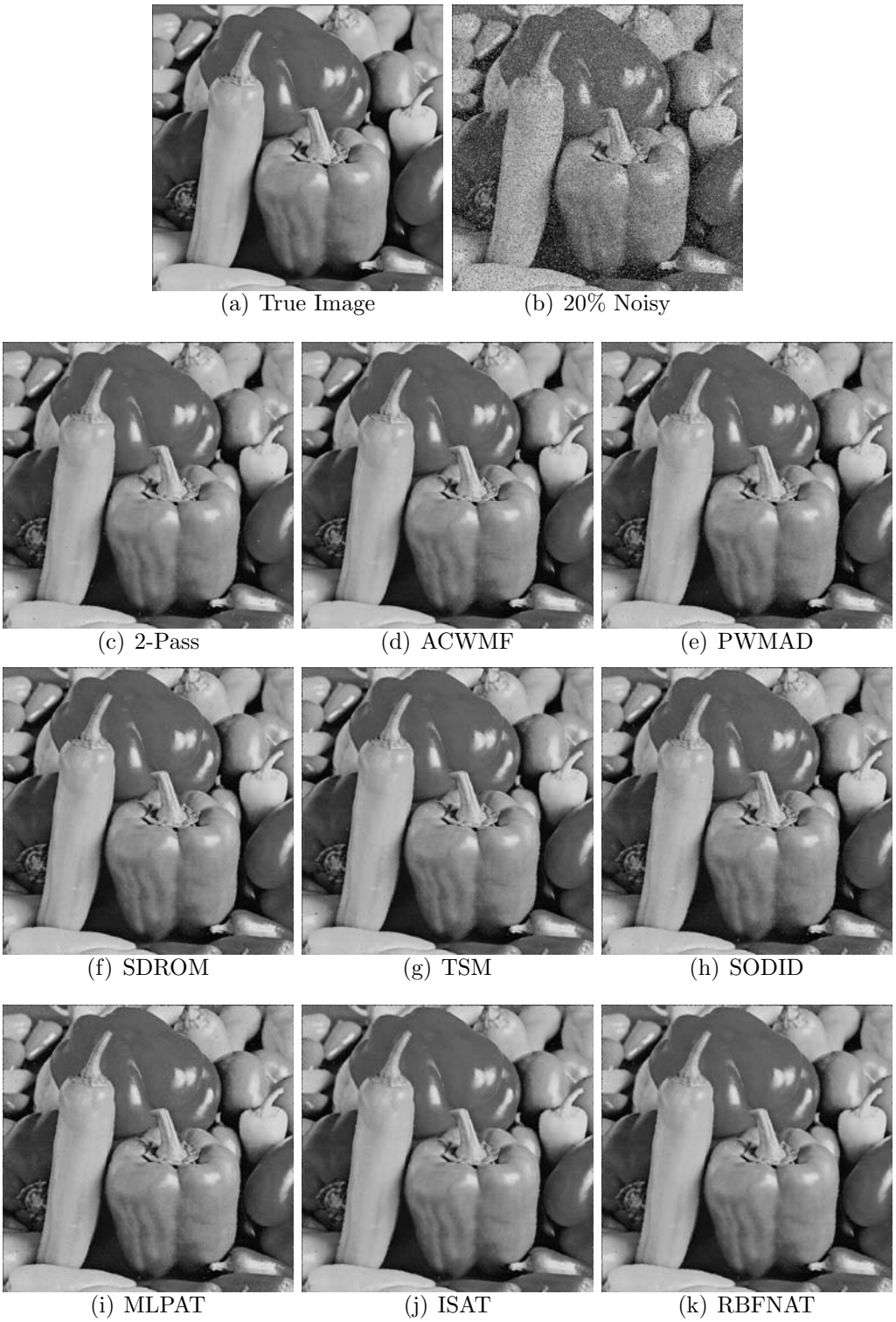

(a) True Image (b) 20% Noisy

(c) 2-Pass (d) ACWMF (e) PWMAD

(f) SDROM (g) TSM (h) SODID

(i) MLPAT (j) ISAT (k) RBFNAT

Figure 2.16: Impulsive Noise filtering of *Peppers* image corrupted with 20% of RVIN by different adaptive threshold schemes

Chapter 3

CV based Adaptive Threshold for Impulsive Noise Detection

In this chapter an improved threshold selection strategy to detect random valued impulsive noise of varying strengths is proposed. The proposed method utilizes another variation of neural network architecture. The method is adaptive in the sense that, the threshold obtained is adaptable to different type of images and noise conditions. The network tuned for one image works for other images as well at different noise conditions. Emphasis is on the use of right kind of statistical parameter to be used as input training pattern. Comparative analysis with other standard techniques reveals that the proposed scheme outperforms its counterparts in terms of noise suppression.

3.1 Methodology

Using the concepts and assumptions in Section 2.1 and 2.2 it can be visualized that the performance of the detection scheme depends upon the threshold value. Successively, threshold value determination depends upon the training parameters. In Chapter 2 two adaptive threshold detection scheme is discussed using two statistical parameters (mean and variance) as the inputs to the neural detectors (MLP, FLANN and RBFN). This chapter introduces a single parameter *Coefficient of Variance*(CV) which can replace the two input parameters (mean and variance) as used in Chapter 2 as an input to the neural detector. Using CV as the input training parameter is explained in the next section. A *Functional Link Artificial neural network* is used for impulse detection using reduced training

parameters in this chapter. The adaptive threshold detection using FLANN and CV as input is described in Section 3.3. Decreasing the training parameters and using an efficient detector i.e. FLANN makes the algorithm work much faster and the network converges faster.

3.2 CV based Adaptive Threshold Detection Algorithm (CVAT)

Many different techniques are used to determine whether a given pixel is affected with impulses or not. Some of these techniques are relatively simple, on other hand some others are complex. Whatever may be the technique, they first determine a threshold and on that basis apply some filtering mechanism. In Chapter 2 three such threshold detection schemes based on neural network have been presented. In this chapter a variation of the previous detection schemes (2.3, 2.5) is being proposed with improved training parameters.

Second order difference (2.1) is utilized here to determine the sanctity of a pixel. Each test pixel is compared with its neighbors in both horizontal and vertical directions. The detected noisy pixel is replaced by the median of the neighboring pixels. The noise detection algorithm of Section 2.1.1 is used here and the adaptive noise threshold is determined as explained in Section 3.3. Since, there cannot be one threshold value, which will be a panacea for different types of images. Hence the threshold should be an adaptive one rather than fixed. Threshold for an image depends on an image environment. Where environment of an image means, the type of image, characteristic of noise and its density. For obtaining a correct threshold some of the image parameters are required. Proper investigation must be carried out to determine the image parameters which can represent it aptly. Steps for selecting the parameters is described below.

Suppose for any image and at a particular noise condition the threshold value θ is varied in a wide range to obtain a set of mean squared error (MSE) values such that a relation can be established. For example:

i. An image (say *Peppers*) is corrupted with impulsive noise of densities 1%,

5%, 10%, 15%, 20%, 25%, and 30%.

ii. The first noisy image $Peppers_1$ (the subscript is for 1% of noise) is subjected to the proposed algorithm outlined in Section 2.1.1 by varying the threshold value θ between 0 and 1.

iii. Corresponding to each θ one mean squared error (MSE) is obtained. The minimum among those MSEs is recorded as $\text{MSE}_{min}^{(Peppers_1)}$. Also the corresponding threshold value is recorded as optimal threshold value θ_{opt}.

iv. Steps (ii) and (iii) are repeated for other noisy *Peppers*, i.e. $Peppers_i$, $i \in \{5, 10, 15, 20, 25, 30\}$.

v. Repeat steps (i) to (iv) for other standard images like *Lena*, *Lisa*, *House*, etc.

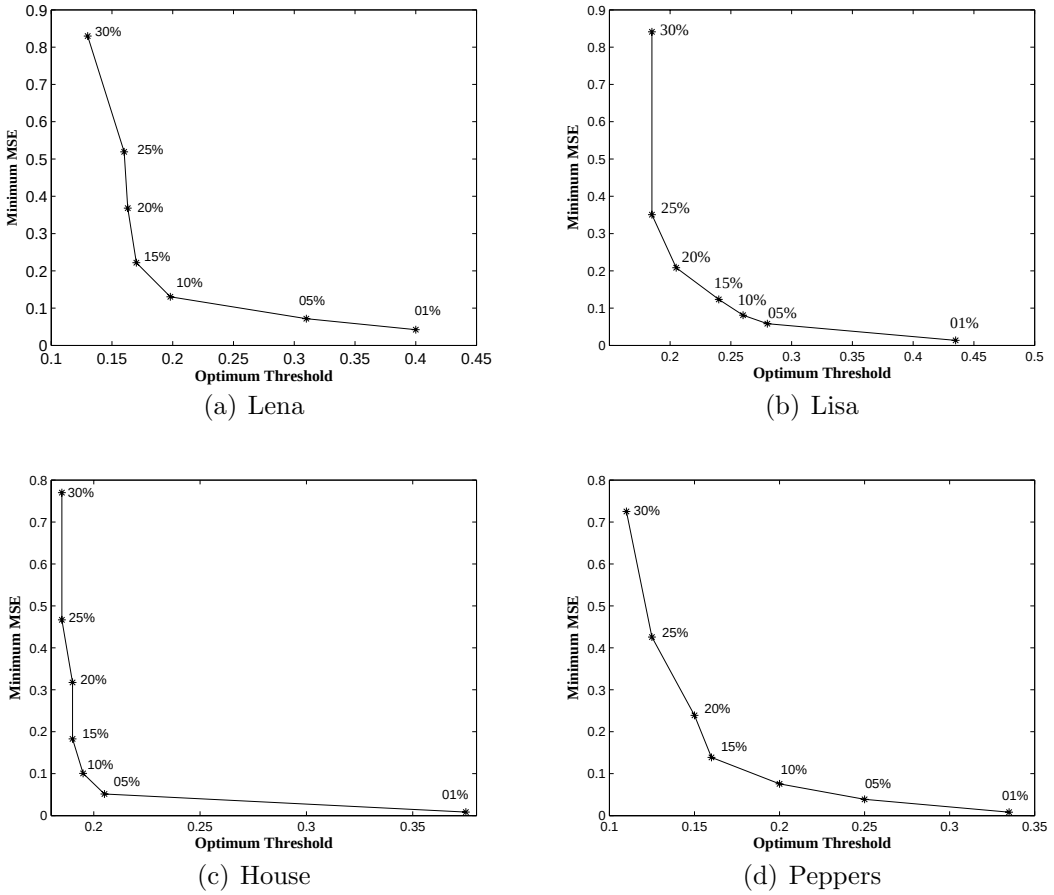

(a) Lena (b) Lisa

(c) House (d) Peppers

Figure 3.1: Variation of Minimum MSE at different Threshold values

Figures 3.1(a), 3.1(b), 3.1(c) and 3.1(d), show the relation between θ_{opt} and MSE_{min} for *Peppers*, *Lena*, *Lisa* and *House* images respectively.

From these plots (Figure 3.1) it is, in general, observed that the minimum MSE and the corresponding threshold bear an exponentially decaying relation. This is true for all other images. In a practical situation, the use of MSE or noise ratio to predict the threshold is ruled out as they need knowledge of the original image for computation. However, to alleviate this problem analysis have been made as follows. The minimum MSE is inversely proportional to optimal threshold value i.e.

$$\text{MSE}_{min} \propto \frac{1}{\theta_{opt}} f \tag{3.1}$$

also the noise percentage is inversely proportional to optimal threshold value, given as:

$$\eta \propto \frac{1}{\theta_{opt}} \tag{3.2}$$

where, η is the noise percentage. Also it is known that:

$$\eta \propto CV \tag{3.3}$$

where,

$$CV = \frac{\sigma}{\mu} \tag{3.4}$$

where, σ and μ are the standard deviation and mean of the noisy image respectively. It should be noticed here that we have used CV instead of mean and variance. Hence the number of input to the neural detector is reduced. The reason of using CV is it is a more useful measure of dispersion in contrast to mean and variance as used in MLPAT, ISAT, RBFNAT as explained in Chapter 2.

From the above four equations(3.1, 3.2, 3.3, 3.4) it may be established that the CV of a noisy image are proportional to the MSE_{min} and hence it can be concluded that CV can be used as an input parameter for threshold selection.

3.3 Improved Adaptive Threshold Selection using FLANN

The proposed improved adaptive threshold selection scheme is based on using efficient input parameters to the neural detector. Functional link Artificial neural Network (FLANN) is a single layer network in which the need of hidden layers is removed and is used here for determining the adaptive threshold. In contrast to the linear weighting of the input pattern produced by the linear links of an MLP, the functional link acts on an element of a pattern or on the entire pattern itself by generating a set of linearly independent functions, and then evaluating these functions with the pattern as the argument [62]. Further, the FLANN structure offers less computational complexity and higher convergence speed than those of an MLP because of its single layer structure. The functional expansion effectively increases the dimensionality of the input vector and hence the hyperplanes generated by the FLANN provides greater discrimination capability in the input pattern space [62, 63]. Hence FLANN is used for applications like function approximation and pattern recognition. The back propagation algorithm, which is used to train the network, becomes very simple because of absence of any hidden layer.

From section 3.2 it was established that the CV can be used as an input training parameter. Hence CV is used as an input to the FLANN in the proposed scheme (CVAT). The proposed neural detector is shown in Figure 3.2. The input CV is functionally expanded in the input layer of FLANN with the trigonometric polynomial basis functions given by:

$$\{1, \mu, sin(\pi \mathrm{CV}), \cdots, sin(N\pi\mu), \mathrm{CV}, cos(\pi \mathrm{CV}), \cdots, cos(N\pi \mathrm{CV})\}$$

The actual output on the output layer is compared with the desired output to determine the error. The weight matrix between the input–output layers is updated using back propagation learning algorithm on the basis of this error. The neural network with trained weights are used to obtain the threshold subsequently. It is observed that FLANN can predict an accurate threshold for images that are not used for training as well.

The threshold value thus obtained is used in the first pass of the algorithm.

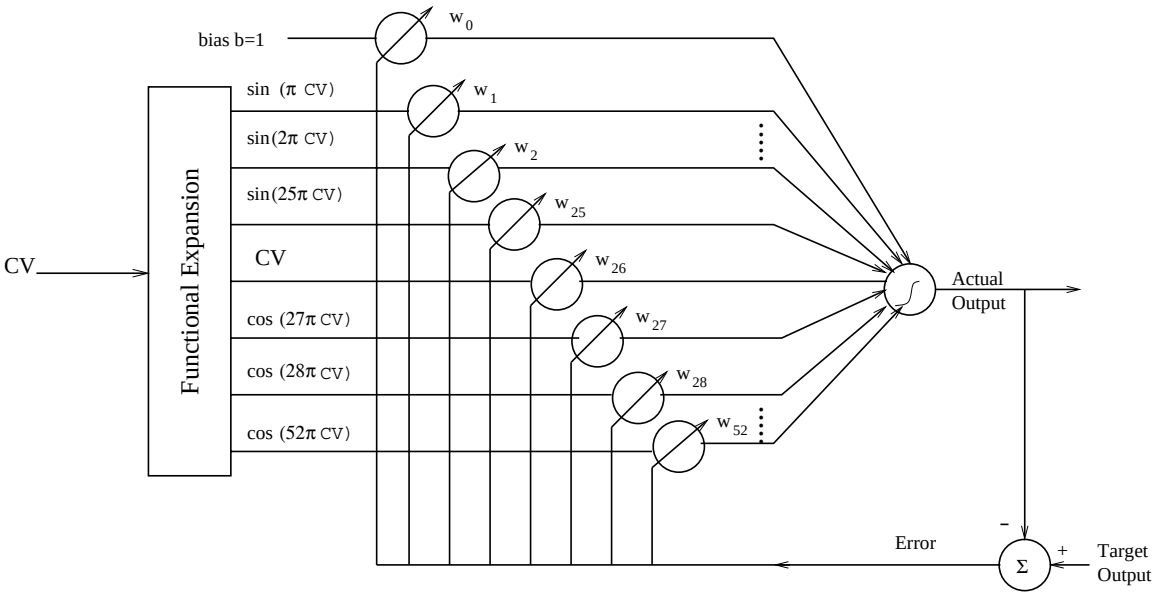

Figure 3.2: Functional Link Artificial Neural Network (FLANN) Structure for Threshold Estimation using CV

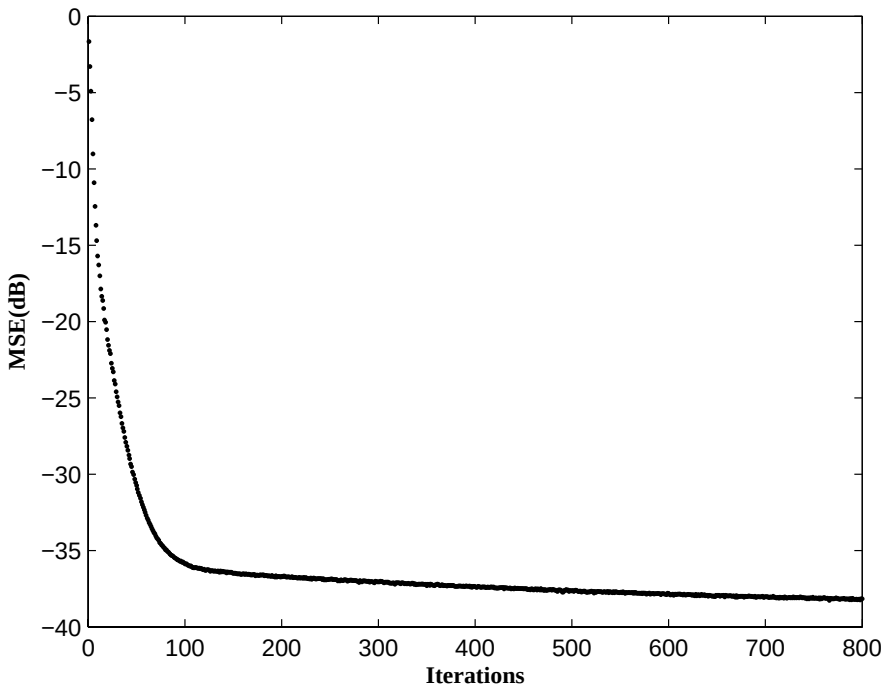

Figure 3.3: Convergence Characteristics of the CV based FLANN

Image output of the first pass is subjected to second pass of the algorithm. A different threshold θ is used in the second pass of the noise detection algorithm. Coefficient of variance (CV) of the output image of the first pass is calculated. This

new CV is again used as input to fed the FLANN to obtain the new threshold value.

3.4 Simulations and Results

The proposed scheme CVAT is simulated on some standard images like *Lena*, *Lisa*, *Girl*, *Clown*, *Gatlin*, *Bridge*, *Boat* and *Peppers* etc. *Lena* image is corrupted with *Random Valued Impulsive Noise* of 1–30% noise densities. It is observed that using a single parameter CV results with faster convergence along with much less computational complexity. This smaller network size because of single input parameter provides better options for easier implementations without hampering noise suppressing capabilities.

The seven noisy images thus generated are passed through the proposed scheme CVAT along with Signal Dependent-Rank Ordered Mean (SD-ROM) [41], Tri-State Median (TSM) [42] and Pixel Wise MAD (PWMAD) [37]. These are the few best performer in terms of noise suppression as discussed in Chapter 1. The simulated result of PSNR (in dB) is plotted in Figure 3.4 and that of PSP (in Percentage) in Figure 3.5.

The computational time required for restoring *Lena* image with each scheme cited above are recorded and is shown in Table 3.3. It is observed that the proposed scheme is computationally much faster with respect to all other few best noise suppression schemes.

Few more comparisons are listed in the form of tables. Table 2.1 lists the PSNR of various images corrupted with 15% and 20% of noise. Similar observations of PSP are listed in Table 3.2.

The figures in 3.6 and 3.7 shows the images of restored *Lena* and restored *Peppers* corrupted with 15% and 20% of noise densities respectively.

3.5 Summary

The proposed scheme is an improved filtering scheme for suppressing impulsive noise of varying strengths from corrupted images. A variation of neural network and with a single parameter adaptive threshold is obtained. The proposed

Table 3.1: PSNR (dB) of different schemes at 15% and 20% of noise on different images

		Lisa	*Girl*	*Clown*	*Gatlin*	*Bridge*	*Boat*	*Peppers*
	PWMAD	30.50	29.28	23.02	30.66	26.07	29.25	31.29
15%	SD-ROM	31.98	31.31	24.33	32.77	27.48	30.75	32.00
RVIN	TSM	32.05	31.05	23.88	32.46	27.08	30.51	33.04
	CVAT	36.45	33.87	23.59	33.16	25.89	28.93	33.11
	PWMAD	28.26	27.73	22.16	28.77	24.99	27.57	29.04
20%	SD-ROM	30.86	29.92	23.59	31.51	26.55	29.50	31.40
RVIN	TSM	30.95	29.69	23.28	31.30	26.28	29.35	31.41
	CVAT	34.68	31.72	22.53	31.60	25.91	28.28	32.57

Table 3.2: PSP of different schemes at 15% and 20% of noise on different images

		Lisa	*Girl*	*Clown*	*Gatlin*	*Bridge*	*Boat*	*Peppers*
	PWMAD	7.35	11.05	24.85	4.00	15.83	13.95	10.53
15%	SD-ROM	0.14	0.93	10.29	0.39	3.06	1.04	0.34
RVIN	TSM	0.22	2.62	17.51	0.98	7.94	2.55	0.57
	CVAT	10.5	16.15	57.82	9.05	36.37	73.61	35.08
	PWMAD	7.06	7.82	22.77	5.03	15.10	13.18	10.05
20%	SD-ROM	0.18	0.40	9.86	0.33	3.10	1.12	0.37
RVIN	TSM	0.31	1.21	21.07	1.00	8.30	2.82	0.73
	CVAT	10.50	16.15	57.82	9.05	0.06	74.21	55.98

Table 3.3: Computational time consumed by different Schemes for removing impulsive noise from *Lena* image corrupted with 15% of RVIN

Scheme	Time (sec)
PWMAD	244.68
SDROM	11.20
TSM	77.14
CVAT	9.32

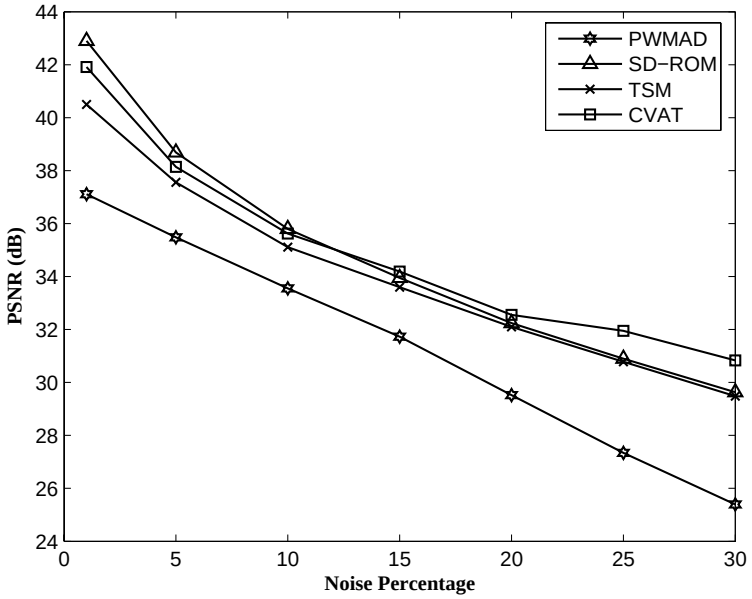

Figure 3.4: PSNR (dB) plot of Restored *Lena* image corrupted with RVIN of varying strengths

schemes' performances are poor when compared with some of the schemes. However, computationally the proposed schemes are well off.

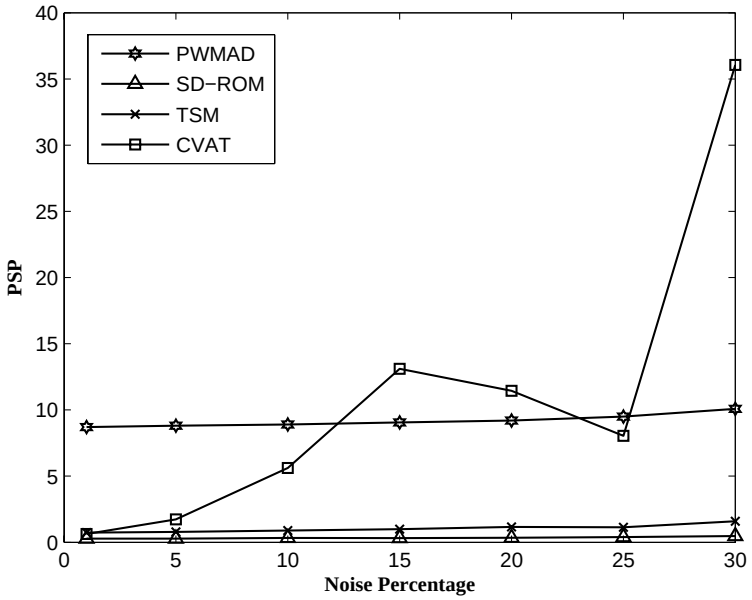

Figure 3.5: PSP plot of Restored *Lena* image corrupted with RVIN of varying strengths

(a) True Image (b) 15% Noisy (c) PWMAD

(d) SDROM (e) TSM (f) CVAT

Figure 3.6: Subjective comparison of impulsive noise removal of *Lena* image corrupted with 15% of RVIN by different filters

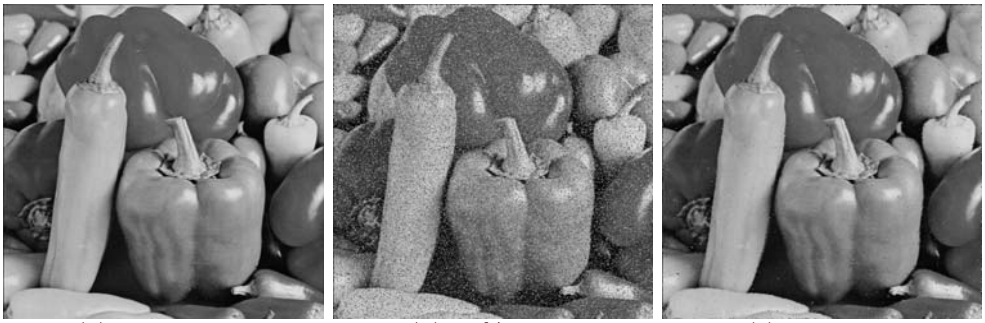

(a) True Image (b) 20% Noisy (c) PWMAD

(d) SDROM (e) TSM (f) CVAT

Figure 3.7: Subjective comparison of impulsive noise removal of *Peppers* image corrupted with 20% of RVIN by different filters

Chapter 4

Comparative Study of Impulsive Noise Suppression Schemes

To combat impulsive noise from images, several schemes have been suggested in the literature as well as in this thesis. In each chapter of this thesis the performance of the proposed method has been compared isolatedly with relevant standard techniques. However the relative performance comparison has not been made amongst the different proposed methods vis-a-vis with the standard methods. The objective of this chapter is to critically study the comparative filtering performance amongst the various methods proposed in this thesis. A conclusion has also been drawn to choose a method for impulsive noise filtering under a particular noise situation. Impulsive noise can be classified into three categories i.e. low, medium and high according to Table 4.1. Studies have been made at different noise conditions. For comparison, all the methods in a particular chapter is selected here and Table 4.2 shows the different filtering scheme chosen from different chapters.

Table 4.1: Noise classification as per noise ratio

Noise Level	Noise Classification
0–15%	Low
15%–30%	Medium
30% and above	High

Table 4.2: Noise removal scheme chosen for comparison

Scheme	Neural Structure	Noise Condition
MLPAT	MLP	Low & Medium
ISAT	FLANN	High
RBFNAT	RBFN	High
CVAT	FLANN	High

In sequel the following analysis is made with regard to the performance evaluation as presented,

- *Detector Capability*
- *Average Filtering performance*
- *Computational Overhead*

4.1 Performance Evaluation based on detector capability

Four different noise detectors i.e. MLPAT, FLANNAT, RBFNAT and CVAT detector have been proposed to detect impulsive noise at a test pixel location based on the gray level information of its neighbor pixels in a 3×3 window. The detector capability for noise classification is performed on the basis of certain performance metrics i.e. False Positive % (FP) and False Negative (FN%) as defined below.

$$FP\% = \frac{\text{number of False Positives}}{\text{Total number of noise free pixels}} \times 100 \tag{4.1}$$

$$FN\% = \frac{\text{number of False Negatives}}{\text{Total number of noisy pixels}} \times 100 \tag{4.2}$$

Where, classification of noise free pixels as noisy is termed as False Positive and classification of noisy pixels as noise free is termed as False Negative. The reported detectors are subjected to this test to determine their noise classification efficiency. The proposed detectors performance in terms of FP% and FN% is compared with PWMAD [37] the best scheme of the literature. The present study has been made

for low and medium noise conditions (less than 30 %). Simulation has been carried out using standard image i.e. *Lena* at 15% noise condition and the computed results are presented in Table 4.3. Comparative analysis of the proposed detectors reveals that CVAT detector yields the best performance in terms of the defined parameter i.e FP% and FN%.

Table 4.3: False Positive Percentage(FP%) and False Negative Percentage (FN%) of proposed schemes for Lena (512×512) with 15% RVIN.

	FP%	FN%
PWMAD	1.69	4.51
MLPAT	1.60	2.18
ISAT	1.64	2.14
RBFNAT	1.42	1.69
CVAT	0.88	1.22

4.2 Comparison of Filtering Performance

Filtering performance of the proposed schemes is measured here with a suitable restoration parameter i.e. PSNR (Section 1.5). The suggested schemes are simulated on standard Lena image with noise levels varied between 1 to 30%. Computed results are compared on the basis of an certain criteria as presented in Table 4.4.PSNR values are computed and used as performance indices for the proposed schemes. The basis of comparison is provided in Table 4.4.

Table 4.4: Basis of comparison among the filtering schemes

Parameter	Range	Remarks
PSNR (dB)	0–15	Satisfactory (S)
	15–30	Good (G)
	30 and above	Excellent (E)

Based on the aforesaid criteria, comparison has been made in two groups: (a) Low and medium noise conditions and (b) high noise conditions. Computed PSNR results obtained from the simulation of different schemes are shown in Table 4.5 and 4.6. The plot in Figure 4.1 shows the PSNR variations of the proposed schemes.

Table 4.5: Comparison of schemes under low and medium noise conditions

Filters	PSNR	Remarks
MLPAT	E	G
ISAT	E	E
RBFNAT	E	E
CVAT	E	E

Table 4.6: Comparison of different schemes under high noise conditions

Filters	PSNR	Remarks
MLPAT	G	S
ISAT	E	E
RBFNAT	E	E
CVAT	E	E

4.3 Computational Overhead

In this section the computational overhead associated with each proposed filter to restore a corrupted pixel is compared. It is evident from the Table 4.7 that the CVAT filtering scheme is the most computationally efficient scheme. The computational time required for restoring Lena image with each proposed scheme

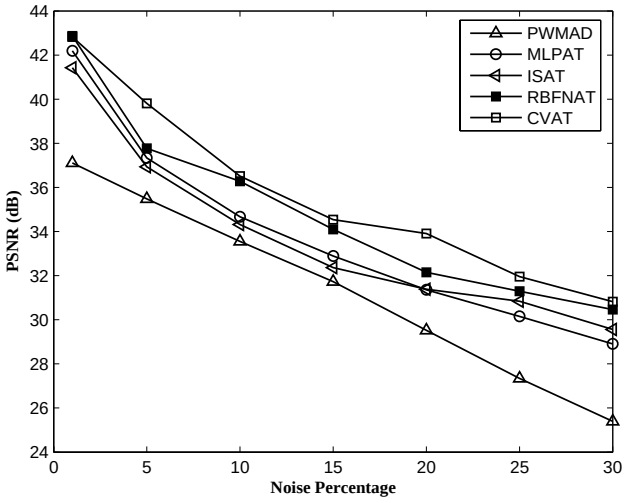

Figure 4.1: Variation of PSNR (dB) at different RVIN percentage on *Lena* image.

along with PWMAD [37] is shown in Figure 4.2. All the results were obtained by simulating the schemes in Matlab 7.0, Microsoft Windows XP (SP2) Operating System and Intel Pentium D–2.80 GHz with 1GB of RAM.

Table 4.7: Computational overhead per pixel associated in filtering schemes

Filters	Addition	Multiplication
MLPAT	7	8
ISAT	4	207
RBFNAT	10	12
CVAT	4	57

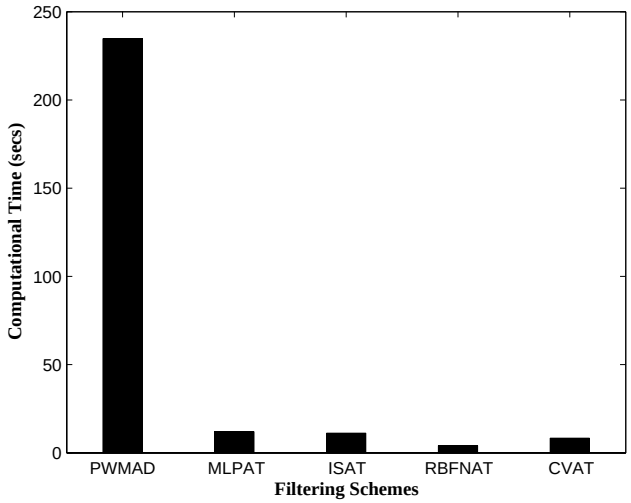

Figure 4.2: Computational time of proposed schemes for *Lena* (512×512) with 15% RVIN.

4.4 Summary

From the results obtained (Table 4.5, 4.6), it is observed that CVAT, RBFNAT, ISAT filtering schemes perform better than MLPAT. But since the CV based FLANN detector used in CVAT filtering scheme outperforms the other schemes, CVAT scheme is chosen to be the best among these methods at all the noise conditions.

In the next chapter, CVAT and RBFNAT filtering schemes are used for image sharpening under impulsive noise condition.

Chapter 5

Image Sharpening under Impulsive Noise Conditions

One of the problems of a image sharpening in practice is the noise boost-up, which limits the applications of the enhancement schemes in low contrast images under noisy conditions. To resolve this issue, a novel approach is presented, which effectively prevents the visual amplification of a noise while the image details are being enhanced. The proposed scheme incorporates noise reduction algorithm before applying contrast enhancement to achieve the objective. Only low contrast images under impulsive noise condition is considered here. RBFNAT(Chapter 2) and CVAT(Chapter 3) are used for reducing noise before enhancement. Image Enhancement scheme used here is based on a technique called *Unsharp Masking*(UM), which is described in Section 5.1. Noise amplification in low contrast noisy images is the major drawback of *linear unsharp masking*. Since sharpening (enhancement) and smoothing (noise removal) are contradicting in nature proper care must be taken to obtain high quality images. This chapter tries to express how selective filtering (Chapter 2, 3) can be applied along with UM to improve the quality of low contrast noisy images. With appropriate choice of impulse noise removal schemes the noise amplification can be prevented, to be employed for UM. *Linear Unsharp Masking* (UM) is presented in Section 5.1. Section 5.2 reports an improved image sharpening scheme under impulsive noise condition. Last, the proposed sharpening scheme is compared with some of the existing schemes and is presented in Section 5.3. Finally, Section 5.4 provides the summary of the chapter.

5.1 Image Enhancement using Unsharp masking

Image enhancement seeks to improve the visual quality of images. However, an inherent difficulty is to define a mathematical criterion for visual quality. As a result, many algorithms remain to a large extent empirical and a final assessment can only be performed by the human observer. *Unsharp Masking* (UM) [1] is a classical simple enhancement scheme which yields pleasant results utilizing an effect called simultaneous contrast. Simultaneous contrast describes the visual phenomenon that the difference in the perceived brightness of neighboring regions depends on the sharpness of the transition. Unsharp Masking is implemented by adding a scaled version of the input image to the image itself to form the enhanced image. The block diagram of Linear Unsharp Masking is illustrated in Figure 5.1.

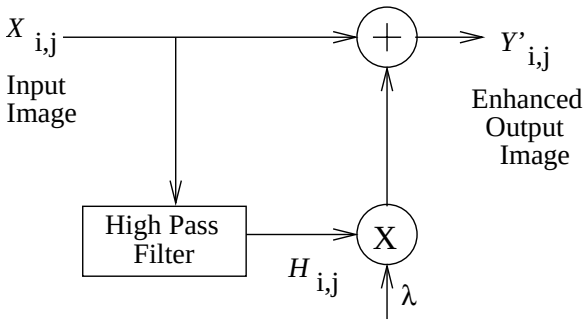

Figure 5.1: Linear Unsharp Masking scheme

5.2 Improved Image sharpening under Impulsive Noise Condition

The proposed image sharpening scheme under noise condition consists of impulse detection followed by simple unsharp masking as described in Section 5.1. The schematic diagram of Improved Unsharp Masking (IUM) scheme is illustrated in Figure 5.2 . To enhance a low contrast noisy image adaptive noise detection schemes (Chapter 2) is used. Initially the noisy pixels are detected followed by median filtering. This type of selective filtering prevents unnecessary blurring of image details and hence image details are preserved even after noise removal. The output of the selective filter is fed to an high pass filter to separate the high and

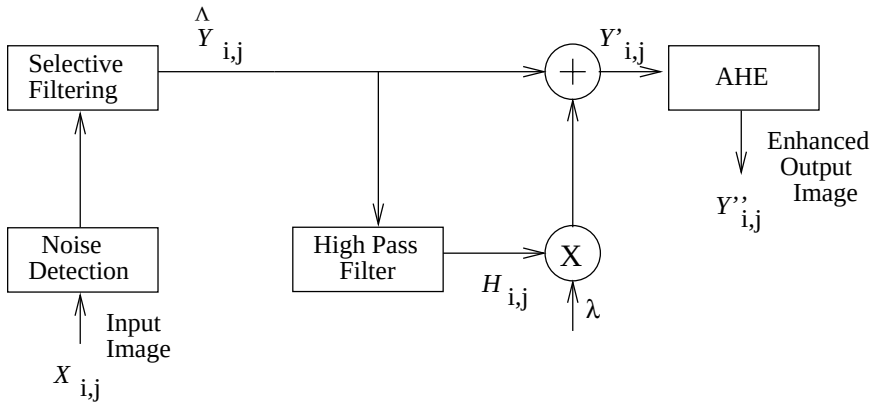

Figure 5.2: Improved Unsharp Masking scheme

low frequency components. Output after selective filtering followed by UM can be expressed using the following relation:

$$Y'_{i,j} = \hat{Y}_{i,j} + \lambda H_{i,j} \tag{5.1}$$

λ is the positive gain factor that controls the level of enhancement. Where $H_{i,j}$ is the output of a linear high pass filter which is obtained using equation 5.2.

$$H_{i,j} = 4\hat{Y}_{i,j} - \hat{Y}_{i-1,j} - \hat{Y}_{i+1,j} - \hat{Y}_{i,j-1} - \hat{Y}_{i,j+1} \tag{5.2}$$

Adaptive Histogram Equalization (AHE) [65] is further applied to redistribute the gray level intensity values of the image uniformly at local level to provide a more sensible image.

5.3 Simulations and Results

The two proposed threshold selection (Chapter 2) schemes were used independently for noise removal before enhancement. The resulting images of noise removal schemes were simulated independently applying UM followed by AHE. Enhanced results were compared with some of the best performing schemes reviewed in Section 1.6.

Since there is no standard quantitative measure because of unavailability of an ideal image, subjective comparison for *Lena* and *Peppers* is presented in Figures 5.3 and 5.4.

5.4 Summary

Problem of noise amplification in image enhancement process is discussed and suitable solution scheme is presented. Use of selective filtering before unsharp masking gives visually accepted results with preserved image details. Two different ways of filtering are used along with unsharp masking to compare the enhanced images. The experimental results demonstrate that the proposed approach can enhance low contrast images under impulse noise condition. Further improvement in the overall enhancement scheme can be achieved by making the amplification factor adaptive.However proposed scheme is not computationally efficient and some parallel processing schemes must be used for real time applications.

(a) Low Contrast Noisy

(b) Linear Unsharp Masking

(c) Median Filtering followed by UM

(d) FLANN followed by UM

(e) RBFN followed by UM

Figure 5.3: Comparison among different enhancement approaches for *Lena image*

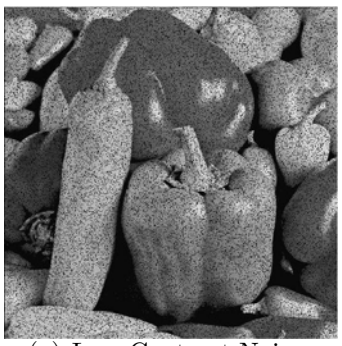

(a) Low Contrast Noisy

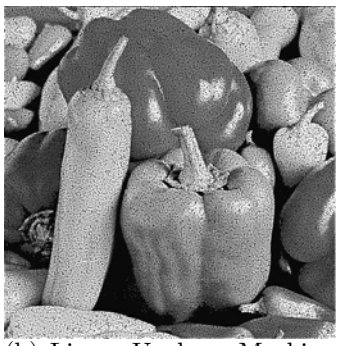

(b) Linear Unsharp Masking

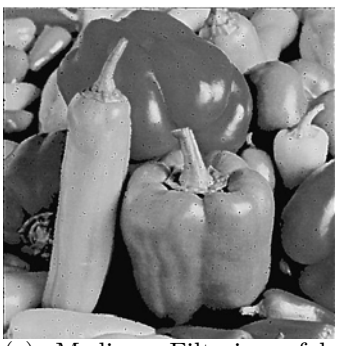

(c) Median Filtering followed by UM

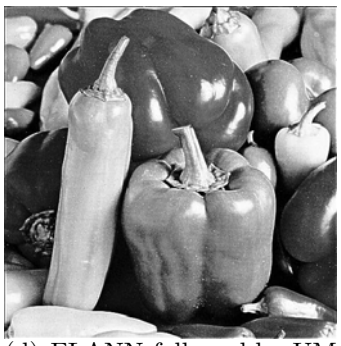

(d) FLANN followed by UM

(e) RBFN followed by UM

Figure 5.4: Comparison among different enhancement approaches for *Pepper image*

Chapter 6
Conclusions

The work in this thesis, primarily focuses on impulsive noise suppression from images. Schemes for adaptive threshold selection for noise detection have also been devised. Along with the above work image sharpening under impulsive noisy condition is also a part of this work.The work reported in this thesis is summarized in this chapter. Section 6.1 lists the pros and cons of the work. Section 6.2 provides some scope for further development.

6.1 Achievements and Limitations of the work

Random Valued Impulsive Noise (RVIN) model is considered in the thesis. Then in subsequent chapters (Chapter 2–3) some novel schemes are proposed. Salient points of the thesis, highlighting the contribution at each stage, are presented below.

The four proposed schemes deal with RVIN removal and are based on second order difference of pixels. These schemes primarily proposes different techniques to select threshold in order to make noise detection process more reliable.

MLP based Adaptive Thresholding for Impulse Detection (MLPAT) is the first contribution that uses a simple Multilayer Perceptron Network (MLP) to determine the threshold value. A variation of ANN i.e. Functional Link ANN (FLANN) is used in another contribution namely *Image Statiscs based Adaptive Threshold Selection for Detecting Impulsive Noise in Images* (ISAT). Radial basis Functional Network (RBFN) is used in another contribution namely *RBFN based Adaptive Threshold Selection for Detecting Impulsive Noise in Images* (RBFNAT). All the

three neural network approach use mean and variance of noisy image as input parameters to the network. Comparisons reveal that there are some better techniques in terms of PSNR. However, the proposed schemes computationally efficient.

In Chapter 3, again the same Functional Link Artificial Neural Network (FLANN) is used in another contribution for detecting impulsive Noise in Images (CVAT). This contribution also deals with removal of RVIN from images. This technique utilizes a more efficient statistical parameter called called coefficient of variance (CV) for training the neural network and to predict the threshold value. In terms of PSNR as well as computational time this scheme outperforms its counterparts.

The last contribution *Image Sharpening under Impulse Noise Condition* suggests an enhancement scheme under noisy conditions. The proposed scheme utilizes selective filtering in improving the pitfalls of an well accepted enhancement allgorithm *Unsharp Masking*. Prevention of noise amplification along with image details preservation while sharpening the proposed scheme outperforms its counterparts in terms of image quality.

6.2 Further Developments

To conclude this thesis, following are some points that may lead to some better and interesting results.

In this thesis, noise detection is mostly covered and for noise filtration median filter is used. Research may be undertaken to devise better filtration techniques. This technique together with a best detection technique can result in optimal restoration of degraded image.

As it has been stated that the existing as well as proposed techniques are computationally expensive, investigation may be carried out in this direction. Development of parallel algorithms can also be done to counter attack the computational overhead.

Bibliography

[1] B. Chanda and D. Dutta Majumder. *Digital Image Processing and Analysis.* Prentice-Hall of India, 1st edition, 2002.

[2] Maria Petrou and Panagiota Bosdogianni. *Image Processing the Fundamentals.* John Wiley and Sons, 1st edition, 1999.

[3] R. C. Gonzalez and R. E. Woods. *Digital Image Processing.* Addison Wesley, 2nd edition, 1992.

[4] Banshidhar Majhi. *Soft Computing Techniques for Image Restoration.* PhD thesis, Sambalpur University, 2000.

[5] S. K. Mitra and T.H. Yu. Nonlinear Filters for Image Sharpening and Smoothing. In *IEEE International Conference on Systems engineering*, volume 4, pages 241 – 244, August 1991.

[6] William K. Pratt. *Digital Image Processing.* John Wiley-Interscience Publication, 3rd edition, 2001.

[7] H. Zhu, F.H. Y. Chan, and F.K. Lam. Image Contrast Enhancement by Constrained Local Histogram Equalisation. *Computer Vision and image Understanding*, 73(2):281 – 290, February 1999.

[8] R.H. Sherrier and GA Johnson. Regionally Adaptive Histogram Equalisation of the Chest. *IEEE Transaction on Medical Imaging*, 6:1 – 7, 1987.

[9] E.P Amburn S.M Pizer. Adaptive Histogram Equalization and its Variations. *Computer Vision, Grpahics, and Image Processing*, 39:355 – 368, 1987.

[10] The NASA Website. http://history.nasa.gov.

[11] The Wikipedia the Free Encylopedia Website. http://en.wikipedia.org.

[12] H. Soltanian-Zadeh, J.P. Windham, and A.E. Yagle. A Multidimensional Nonlinear Edge-Preserving Filter for Magnetic Resonance Image Restoration. *IEEE Transactions on Image Processing*, 4(2):147 – 161, February 1995.

[13] J. A. Goyette, G. D. Lapin, M. G. Kang, and A. K. Katsaggelos. Improving Autoradiograph Resolution Using Image Restoration Techniques. *IEEE Engineering in Medicine Biology*, pages 571 – 574, August/September 1994.

[14] Chieh Ju Tu, Shuen Huei Guan, Yung Yu Chuang, Jiann Rong Wu, Bing Yu Chen, and Ming Ouhyoungi. International Conference on Computer Graphics and Interactive Techniques. SIGGRAPH-2007, San Diego California, 2007.

[15] The Walt Disney Company Website. http://disney.go.com.

[16] Mark R. Banham and Aggleos K. Katsaggelos. Digital Image Restoration. *IEEE Signal Processing Magazine*, 14(2):24 – 41, March 1997.

[17] T.P. ORourke and R.L. Stevenson. Improved Image Decompression for Reduced Transform Coding Artifacts. *IEEE Transactions on Circuits and Systems for Video Technology*, 5(6):490 – 499, December 1995.

[18] T. Ozcelik, J.C. Brailean, and A.K. Katsaggelos. Image and Video Compression Algorithms Based on Recovery Techniques Using Mean Field Annealing. In *IEEE Proceedings*, pages 304 – 316, February 1995.

[19] X. Lee, Y.Q. Zhang, and A. Leon-Garcia. Information Loss Recovery for Block-Based Image Coding Techniques-A Fuzzy Logic Approach. *IEEE Transactions on Image Processing*, 4(3):259 – 273, March 1995.

[20] S. Iyer and S. V. Gogawale. Image Enhancement and Restoration Techniques in Digital Image Processing. *Computer Society of India Communications*, pages 6 – 14, June 1996.

[21] I.Pitas and A.N.Venetsanopoulos. *Nonlinear Digital Filters: Principles and Applications*. Kluwer Academic Publishers, 1990.

[22] J. G. Proakis and D. G. Manolakis. *Digital Signal Processing: Principles, Algorithms and Applications*. Prentice Hall of India, New Delhi, 3rd edition, 2002.

[23] J.Astola and P.Kuosmanen. *Fundamentals of Nonlinear Filtering*. CRC Press, 1997.

[24] R. Bose. *Information Theory Coding and Cryptography*. TATA Mc-Graw Hill, India, 2003.

[25] O.A Ojo and T.G.K. Spassova. An Algorithm for Integrated Noise Reduction and Sharpness Enhancement. *IEEE Transaction on Consumer Electronics*, 46(3):474 – 480, August 2000.

[26] M. Vehvilainen and J. Yrjanainen. Circuit Arrangement to Accentuate the Sharpness and Attenuate the Noise of a Television Image. *In European Patent EP95101009*, 11, February 1994.

[27] Marshall N.W. A comparison between objective and subjective image quality measurements for a full field digital mammography system. *Physics in Medicine and Biology*, 51(10):2441 – 2463, 2006.

[28] S. J. Ko and Y. H. Lee. Center Weighted Median Filters and Their Applications to Image Enhancement. *IEEE Transactions on Circuits and Systems*, 38(9):984 – 993, September 1991.

[29] T. Chen and H. R. Wu. Adaptive Impulse Detection Using Center-Weighted Median Filters. *IEEE Signal Processing Letters*, 8(1):1 – 3, January 2001.

[30] D. R. K. Brownrigg. The Weighted Median Filter. *Communications ACM*, 27:807 – 818, August 1984.

[31] B. I. Justusson. *Median Filtering: Statistical Properties*. Two-Dimensional Signal Processing-II, T. S. Hwang Ed. New York: Springer Verlag, 1981.

[32] E. Abreu, M. Lightstone, S. K. Mitra, and K Arakawa. A New Efficient Approach for the Removal of Impulse Noise from Highly Corrupted Images. *IEEE Transactions on Image Processing*, 5(6):1012 – 1025, June 1996.

[33] Z. Wang and D. Zhang. Progressive Switching Median Filter for the Removal of Impulse Noise from Highly Corrupted Images. *IEEE Transactions on Circuits and Systems–II: Analog and Digital Signal Processing*, 46(1):78 – 80, January 1999.

[34] K. Kondo, M. Haseyama, and H. Kitajima. An Accurate Noise Detector for Image Restoration. In *Proceedings of International Conference on Image Processing 2002*, volume 1, pages I–321 – I–324, September 2002.

[35] S. Zhang and Md. A. Karim. A New Impulse Detector for Switching Median Filters. *IEEE Signal Processing Letters*, 9(11):360 – 363, November 2002.

[36] C. Butakoff and I. Aizenberg. Effective Impulse Detector Based on Rank-Order Criteria. *IEEE Signal Processing Letters*, 11(3):363 – 366, March 2004.

[37] V. Crnojevic, V. Senk, and Z. Trpovski. Advanced Impulse Detection Based on Pixel-Wise MAD. *IEEE Signal Processing Letters*, 11(7):589 – 592, July 2004.

[38] W. Y. Han and J. C. Lin. Minimum-Maximum Exclusive Mean (MMEM) Filter to Remove Impulse Noise from Highly Corrupted Images. *Electronics Letters*, 33(2):124 – 125, January 1997.

[39] P. S. Windyga. Fast Impulsive Noise Removal. *IEEE Transactions on Image Processing*, 10(1):173 – 179, January 2001.

[40] Naif Alajlan, Mohamed Kamel, and Ed Jernigan. Detail Preserving Impulsive Noise Removal. *Signal Processing: Image Communication*, 19:993 – 1003, 2004.

[41] E. Abreu and S. K. Mitra. A Signal-Dependent Rank Ordered Mean (SD-ROM) filter-A new approach for removal of impulses from highly corrupted

images. In *Proceedings of International Conference on Acoustics, Speech, and Signal Processing*, volume 4 of *ICASSP-95*, pages 2371 – 2374, May 1995.

[42] T. Chen, K. K. Ma, and L. H. Chen. Tri-State Median Filter for Image Denoising. *IEEE Transactions on Image Processing*, 8(12):1834 – 1838, December 1999.

[43] F. Russo. Impulse Noise Cancellation in Image Data Using A Two-Output Nonlinear Filter. *Measurement*, 36:205 – 213, 2004.

[44] L. Khriji and M. Gabbouj. Median-Rational Hybrid Filters. In *Proceedings of International Conference on Image Processing 1998*, volume 2, pages 853 – 857, October 1998.

[45] Tuncer Can Aysal and Kenneth E. Barner. Generalized Mean Median Filtering for Robust Frequency Selective Applications. *IEEE Transactions on Signal Processing*, 55(3):937 – 948, March 2007.

[46] P. Maragos and R.W. Schafer. Morphological Filters Part–i: Their Set Theoritic Analysis and Relations to Linear Shift Invariant Filters. *IEEE Transactions on Accoustics, Speech, Signal process*, 35(8):1152 – 1169, June 1987.

[47] A. Polesel, G.Ramponi, and V.J. Mathews. Adaptive Unsharp Masking for Contrast Enhancement. *IEEE Transactions on Consumer Electronics*, 1:267 – 270, 1997.

[48] B. Picinbono. Quadratic Filters. *IEEE Transactions on Accoustics, Speech and Signal Processing IEEE International Conference on ICASSP*, 7(8):298 – 301, May 1982.

[49] S. Thurnhofer and S. K. Mitra. A general framework for quadratic volterra filters. *IEEE Transactions on Image Processing*, 5(6):950 – 963, June 1996.

[50] M.A. Badamchizadeh and A. Aghagolzadeh.

[51] A. Polesel, G.Ramponi, and V.J. Mathews. Adaptive Unsharp Masking for Contrast Enhancement. *IEEE Transactions on Consumer Electronics*, 1:267 – 270, 1997.

[52] M.Vehvilainen and J.Yrjanainen. Circuit Arrangement to Accentuate the Sharpness and Attentuanate the Noise of Television Image, February 1994.

[53] G.A Mastin. Adaptive filters for digital image noise smoothing. *Computer Vision, Grpahics, and Image Processing*, 31:103 – 121, 1985.

[54] R. M. Haralick and L.G Shapiro. *Digital Image Processing.* Addison Wesley, 1992.

[55] Marco Fischer, Jose L. Paredes, and Gonzalo R. Arce. Weighted median image sharpeners for the world wide webl. *IEEE Transactions on Image Processing*, 11(7):717 – 727, July 2002.

[56] T.C. Ayasal and K.E. Barner. Quadratic Weighted Median Filters for Edge Enhancement of Noisy Images. *IEEE Transactions on Image Processing*, 15(11):3294 – 3301, November 2006.

[57] X. Xu and E. L. Miller. Adaptive Two-Pass Median Filter to Remove Impulsive Noise. In *Proceedings of International Conference on Image Processing 2002*, pages I–808 – I–811, September 2002.

[58] F. Russo and G. Ramponi. A Fuzzy Filter for Images Corrupted by Impulse Noise. *IEEE Signal Processing Letters*, 3(6):168 – 170, June 1996.

[59] B.Yegnanarayana. *Artificial Neural Networks.* Prentice-Hall of India, 2003.

[60] V. Kecman. *Learning and Soft Computing.* Pearson Education India, 1st edition, 2004.

[61] Simon Haykin. *Neural Networks.* Prentice Hall, 2nd edition, 1999.

[62] J. C. Patra, R. N. Pal, B. N. Chatterji, and G. Panda. Identification of Nonlinear Dynamic Systems Using Functional Link Artificial Neural Networks.

IEEE Transaction on Systems, Man, and Cybernatics, 29(2):254 – 262, April 1999.

[63] J. C. Patra, G. Panda, and R. Baliarsingh. Artificial Neural Network-Based Nonlinearity Estimation of Pressure Sensors. *IEEE Transaction on Instrumentation and Measurement*, 43(6):874 – 881, December 1994.

[64] Banshidhar Majhi, Pankaj Kumar Sa, and Ganapati Panda. Second Order Differential Impulse Detector. In *IEE International Conference on Intelligent Systems*, ICIS-2005, Malaysia, December 2005.

[65] G.D Hann. Memory Integrated Noise Reduction for Television. *IEEE Transactions on Consumer Electronics*, 42(2):175 – 181, May 1996.

Dissemination of Work

Published

1. S. Mohapatra, R. Dash, P. K. Sa and B. Majhi, ‟Improved enhancement scheme using a RBFN detector for impulse noise.″, *In IEEE International Conference on Emerging Trends in Engineering and Technology (ICETET-2008)*, pp 294 - 297, 16 - 18 July, 2008, Nagpur, India.

2. S. Mohapatra, R. Dash, P. K. Sa and B. Majhi, ‟RBFN based Impulsive Noise Removal Image Enhancement Technique″, *IEEE Conference on Computational Intelligence, Control And Computer Vision in Robotics and Automation, (CICCVRA-2008)*, pp 130 - 135, 10 - 11 March, 2008, Rourkela, India.

3. S. Mohapatra, P. K. Sa and B. Majhi,, ‟Impulsive Noise Removal Image Enhancement Technique″, *6th WSEAS International Conference on Circuits, Systems, Electronics, Control and Signal Processing,, (CSECS-2007)*, pp 317 - 322, 29 - 31 December, 2007, Cairo, Egypt.

4. S. Mohapatra, P. K. Sa and B. Majhi,, ‟An Improved Image Enhancement Technique Combining Sharpening and Impulse Noise Reduction.″, *International Conference on Soft Computing and Intelligent Systems, (ICSCIS-2007)*, pp 317 - 322, 27 - 29 December, 2007, Jabalpur, India.

5. S. Mohapatra, P. K. Sa and B. Majhi,, ‟CV based adaptive threshold selection for impulsive noise removal from images.″, *2nd International conference on Advanced Computing and Communication Technologies, (ICACCT-2007)*, pp 307 - 312, 03 - 04 November, 2007, Panipat, India.

Communicated

1. S. Mohapatra, R. Dash, P. K. Sa and B. Majhi, "Adaptive threshold selection for impulse noise detection in images using coefficient of variance", *International Journal of Neural Computing and Applications*.